# COLLIDERS

D. Treille
CERN, Geneva, Switzerland

**Abstract**

Some themes of collider physics, for the near and for the more remote future, are developed.

## 1 INTRODUCTION

Dealing with colliders in one hour is an almost impossible task! Let me develop a selection of ideas — and try to convey optimism and incentives for the future.

Colliders dominate particle physics at the present time and this will continue in the years to come, with the Stanford Linear Collider (SLC), the Large Electron–Positron (LEP) collider, HERA, the Tevatron etc. They are the key of the more remote future, with the Large Hadron Collider (LHC) about ten years from now, and a Linear Collider, more difficult to locate in time. Lower energy options (B factories, under construction, ...) or possible versions not yet considered in depth ($Z^0$ factory, ...) should also play crucial roles.

These machines will provide a variety of types of collisions: $e^+e^-$, ep, pp or $p\bar{p}$, ion collisions. Altogether they will allow the performance of a vast programme of direct searches, covering most of the foreseeable physics scenarios, as well as a set of accurate measurements, which, compared to the Standard Model (SM) expectations, should be a powerful and complementary discloser of new phenomena.

These main scenarios, going beyond the SM, are well known and documented and I shall only review them briefly. One should, however, always keep in mind the possible occurrence of the unexpected and, rather than focusing on sharply defined physics channels, one should consider broad classes of potentially interesting final states and optimize the experimentation accordingly.

The general features and promises of $e^+e^-$ and hadron colliders are well known and quite contrasted, as illustrated by Fig. 1 [1].

Hadron machines provide broadband beams of partons, and the luminosity of elementary collisions at an effective $\sqrt{s}$ depends both on the luminosity and on the energy of the machine. As a rule of thumb, for an effective $\sqrt{s} \sim 1$ TeV, an order of magnitude in the luminosity of the parent collision is worth a factor $\sim 3$ in their energy: however, one can easily invent counterexamples, for which what really matters is the energy.

As for $e^+e^-$ machines, they provide a sharp peak of luminosity of elementary $e^+e^-$ collisions, at the maximum energy, with some tail towards lower $E$ due to radiation phenomena (brems- and beamstrahlung). But they also deliver broadband beams of radiated electroweak bosons. The domain of $\gamma\gamma$ collisions is well known. At high energies WW collisions, among others, and in particular their longitudinal components, will play an important role. One sees that the LHC and a TeV $e^+e^-$ collider are roughly equivalent in this respect.

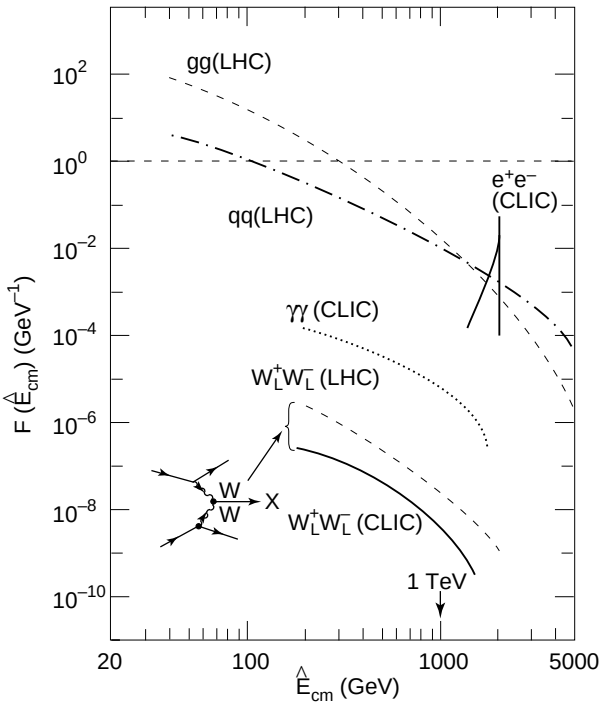


Figure 1: Parton–parton normalized luminosities at the LHC and CLIC (i.e. a TeV collider) (see Ref. [1] for details).

## 2 THE MACHINES IN BRIEF

### 2.1 The present

One can find a summary of the status of present machines in Ref. [2]

The e–p colliding ring HERA is progressively increasing its luminosity. The polarization of $e^-$ is reaching 60%. A fixed-target programme, HERA B, to be run on the proton ring by 1999, is intended to measure CP violation in the B sector.

The $e^+e^-$ collider SLC, prototype of a linear one, is approaching its nominal luminosity. The rate of accumulated $Z^0$'s is relatively low ($\sim$ 150 000) but a very high level ($\sim$ 80%) of longitudinal polarization of the $e^-$ is available and exploited. The value of the polarization must, however, be measured by Compton and Møller scattering.

The $p\bar{p}$ Tevatron collider has accumulated $\sim$ 110 $pb^{-1}$. The CDF and D0 experiments have observed the top quark and given its mass within $\sim \pm 12$ GeV. The accuracy on $m_W$ is also gradually improving. In 1999 or so a major upgrade, through a new injector, is foreseen. The Tevatron should then deliver $\sim$ 15 $pb^{-1}$/week, so that one can expect an accumulation of $\sim$ 1 $fb^{-1}$ in the first years of the 21st century. The possibility of a further

upgrade (TeV$\star$), to reach an order of magnitude more luminosity, is also being considered by some authors.

At LEP full priority is now being given to the energy rise.

The first phase of LEP, at the $Z^0$ energy, was quite successful and provided $\sim 16$ M $Z^0$'s to the four experiments. The luminosity of a circular electron collider is given by:

$$L = f\, n_{\rm b} \frac{N_{\rm b}^2}{4\pi\sigma_x\sigma_y}$$

where $f$ is the rotation frequency, $N_{\rm b}$ the number of particles per bunch, and the denominator is the transverse area of the interaction region. The only 'free' parameter is the number of bunches per beam, $n_{\rm b}$. It was four at the start of LEP and much activity was devoted to raising that number while avoiding unwanted collisions. A 'pretzel' configuration [3] with eight bunches provided up to $L_{\rm peak} = 2.2 \times 10^{31}$ cm$^{-2}$s$^{-1}$. More recently a bunch train solution, with $n_{\rm b} = 4 \times n$, $n = 2, 3, 4$, was exploited.

The integrated luminosity per year has been rising regularly. In 1994 it was 65 pb$^{-1}$/ experiment.

Transverse polarization, due to the 'natural' Sokolov–Ternov effect and maintained against depolarization resonances by harmonic spin-matching techniques, has reached a level of $\sim 40\%$. It has been shown that it was kept when beams were interacting.

It was extensively used, through a resonant depolarization method, for ultraprecise measurement of the beam energy. The method itself gives an accuracy better than a MeV, much less than the beam energy spread. This is understandable since the depolarization time is long compared to the energy oscillation time of a particle, so that the relevant energy is the average one.

This calibration was the key to the very accurate determination of $m_{\rm Z}$ and $\Gamma_{\rm Z}$ ($\sim 2$ and $\sim 3$ MeV, respectively, as preliminary values).

It has revealed spectacular correlations of LEP energy with the tidal force, the level of water in the Lake of Geneva, and the timetable of the electric trains passing by (Fig. 2). LEP has written there a beautiful chapter of machine physics, which is not yet fully closed.

It is potentially possible to turn the transverse into a longitudinal polarization and use it for physics, in particular for the $A_{\rm LR}$ measurement. The advantage of LEP would be that both $e^-$ and $e^+$ are polarized. By using the trick of a selective action on the polarization of individual bunches, one can then measure the level of polarization by a simple counting of $Z^0$'s. Such a programme, studied in detail in Ref. [4] will, however, not occur before LEP 200. Results from polarized collisions are actually coming from the SLC.

### 2.2 LEP 200

The overall problem for LEP 200 is well known. The energy loss per turn due to synchrotron radiation goes like the fourth power of the energy and will reach 2.5 GeV for a beam energy of 100 GeV. Besides the increased background problems, solved by appropriate masking of the experiments, one has to compensate for that loss by providing the necessary accelerating voltage around the ring. This is done by RF cavities: the warm copper cavities of LEP I are totally insufficient and one had to develop and realize a large set of superconducting ones, made of copper with an internal layer of sputtered niobium.

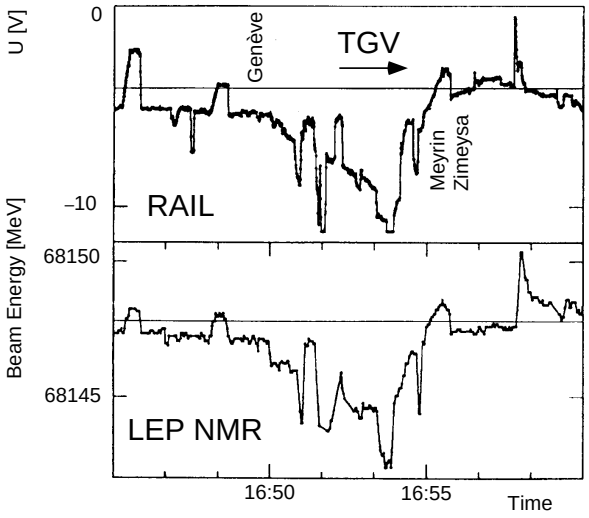


Figure 2: Correlation in time between trains and the LEP NMR.

This programme turned out to be very challenging. Besides the cavities themselves, the main couplers, feeding in the RF power, and the higher order mode couplers, filtering out selectively the bad harmonics, were critical items. After solving a series of problems, it is now foreseen that an accelerating field of 6 MV/m with a quality factor of a least $3.2 \times 10^9$ should be achieved by the set of cavities. Further improvements may be possible ultimately.

One can then deduce the number of cavities needed to reach a given beam energy. Besides the financial ones, there exist practical limitations to the amount of cavities one can install around LEP. It is out of the question to undertake new massive civil engineering and so one must manage with the room available in the existing galleries of the four even-numbered straight sections: the corresponding limit is around 352 cavities, and can be raised to around 384 cavities by removing the separators needed for bunch train operation. Furthermore, at each point, there is currently a cryogenic limit amounting to about 12 kW: the exact number of cavities which can be accommodated locally will depend on the cryogenic load they represent. Beyond that number (72 to 80 cavities?) one would have to increase the cryogenic power, a step anyway needed for the LHC.

Table 1 [5] gives the details of the possible scenarios. Scenario IV can now be considered as approved. One sees from the table that up to $\sqrt{s} \sim 205$ (i.e. except for the ultimate Z scenario) one can work with $4 \times 2$ bunch trains, providing a peak luminosity of nearly $10^{32}\,\mathrm{cm}^{-2}\,\mathrm{s}^{-1}$.

Should one multiply this value by $10^7$ s (a 'year') one would expect close to 1000 $\mathrm{pb}^{-1}$ per 'year' per experiment. This is, however, an unrealistic number and, guided by the present LEP achievements and the conditions expected at LEP 200, one has adopted a value of $\sim 170\,\mathrm{pb}^{-1}$ per 'year' per experiment which leads to $\sim 500\,\mathrm{pb}^{-1}$ in 3 years.

Since for some physics channels it is likely that the four experiments will combine their results, one can also consider the 'quantum' of 1 $\mathrm{fb}^{-1}$, which represents the total luminosity delivered in around 1.5 years.

A first exposure of $\sim 6\,\mathrm{pb}^{-1}$ has recently been performed at 130–136 GeV c.m. energy. The run went smoothly, and is another success of the LEP machine.

## Table 1

| Point No. / Type | Cavities: 2 Cu | 2 Nb | 2 NbCu | 4 NbCu | 6 Cu | 6 NbCu | 8 NbCu | Totals Cu | Totals Nb | Totals NbCu | Missing cavities | Total (MV) | $\ell_{max}$ (mA) | $\xi_{bb}$ | Beam power (MW) |
|---|---|---|---|---|---|---|---|---|---|---|---|---|---|---|---|
| Phase II | 60 | 32 | 0 | 64 | 60 | 32 | 64 | 120 | 32 | 160 | 0 | 2243 | 6.00 | 0.0335 | 24.3 |
| Original LEP2 'Design' | | | | | | | | | | | 8 | 2161 | 6.00 | 0.0340 | 23.3 |
| | | | | | | | | | | | 16 | 2080 | 6.00 | 0.0350 | 22.7 |
| III | 28 | 32 | 16 | 64 | 28 | 48 | 64 | 56 | 32 | 192 | 0 | 2390 | 6.60 | 0.0355 | 28.6 |
| Upgrade for increased luminosity | | | | | | | | | | | 8 | 2308 | 6.90 | 0.0380 | 28.6 |
| | | | | | | | | | | | 16 | 2227 | 7.20 | 0.0400 | 28.6 |
| IIIa | 26 | 32 | 24 | 56 | 26 | 56 | 56 | 52 | 32 | 192 | 0 | | | | |
| Modifications for bunch trains | | | | | | | | | | | 8 | | | Almost identical to pre | |
| | | | | | | | | | | | 16 | | | | |
| IIIb | 26 | 32 | 32 | 56 | 26 | 64 | 56 | 52 | 32 | 208 | 0 | 2542 | 6.70 | 0.0345 | 30.5 |
| Use of 16 active spares (yet to be approved) | | | | | | | | | | | 8 | 2460 | 6.90 | 0.0360 | 30.5 |
| | | | | | | | | | | | 16 | 2379 | 7.10 | 0.0370 | 30.5 |
| IV | 26 | 32 | 32 | 72 | 26 | 64 | 72 | 52 | 32 | 240 | 0 | 2869 | 6.80 | 0.0310 | 34.5 |
| Maximum energy upgrade with $4 \times 12$ kW cryogenics | | | | | | | | | | | 8 | 2787 | 6.90 | 0.0320 | 34.5 |
| | | | | | | | | | | | 16 | 2706 | 7.05 | 0.0340 | 34.5 |
| X1 | 26 | 32 | 32 | 88 | 26 | 64 | 88 | 52 | 32 | 272 | 0 | 3196 | 6.70 | 0.0280 | 38.5 |
| 18 kW cryo at pts 4 and 8 | | | | | | | | | | | 16 | 3032 | 7.10 | 0.0310 | 38.5 |
| X2 | 0 | 32 | 48 | 88 | 0 | 80 | 88 | 0 | 32 | 304 | 0 | 3377 | 6.90 | 0.0280 | 42.0 |
| 18 kW at pts 2 and 6 | | | | | | | | | | | 16 | 3213 | 7.30 | 0.0310 | 42.0 |
| Y | 0 | 32 | 56 | 88 | 0 | 88 | 88 | 0 | 32 | 320 | 0 | 3540 | 6.92 | 0.0270 | 44.0 |
| Symmetrical LEP with all even points identical | | | | | | | | | | | 16 | 3377 | 7.34 | 0.0300 | 44.0 |
| Z | 0 | 32 | 64 | 96 | 0 | 96 | 96 | 0 | 32 | 352 | 0 | 3866 | 4.00 | 0.0300 | 27.5 |
| Ultimate number of cavities with ZL's removed (4 bunches) | | | | | | | | | | | 16 | 3703 | 4.00 | 0.0303 | 26.4 |

* in $cm^{-2}\ s^{-1}$

## 2.3 Linear colliders

A complete set of articles about all aspects of linear collider problems can be found in Ref. [6].

### *2.3.1 Which machines?*

Table 2 gives the main parameters of the Linear Colliders (LCs) under consideration for $\sqrt{s} = 500$ GeV and for which I will use the generic name of NLC (Next Linear Collider).

**Table 2**

| Linear Colliders | CLIC | DLC | JLC | NLC | TESLA | VLEPP |
|---|---|---|---|---|---|---|
| $\mathcal{L}\,[10^{33}\,\mathrm{cm}^{-2}\,\mathrm{s}^{-1}]$ | 2.7 | 2.4 | 6.8 | 6.0 | 2.6 | 12 |
| $f_{\mathrm{rep}}\,[\mathrm{Hz}]$ | 1700 | 50 | 150 | 180 | 10 | 300 |
| $n_{\mathrm{b}}$ | 4 | 172 | 90 | 90 | 800 | 1 |
| $\mathcal{L}_1\,[10^{-3}\,\mathrm{nb}^{-1}]$ | 0.40 | 0.27 | 0.50 | 0.37 | 0.33 | 40 |
| $N\,[10^{10}]$ | 0.6 | 2.1 | 0.7 | 0.65 | 5.15 | 20 |
| $\sigma_x/\sigma_y\,[\mathrm{nm}]$ | 90/8 | 400/32 | 260/3 | 300/3 | 640/100 | 2000/4 |
| $\sigma_z\,[\mu\mathrm{m}]$ | 170 | 500 | 80 | 100 | 1000 | 750 |
| $\beta_x^*/\beta_y^*\,[\mathrm{mm}]$ | 2.2/0.16 | 16/1 | 10/0.1 | 10/0.1 | 10/5 | 100/0.1 |
| $D_x/D_y$ | 1.3/15 | 0.70/8.8 | 0.09/8.2 | 0.08/8.2 | 1.25/8.0 | 0.43/– |
| $A_x/A_y$ | 0.08/1.06 | 0.03/0.5 | 0.008/0.8 | 0.01/1.0 | 0.1/0.2 | 0.008/– |
| $\bar{\sigma}_x/\bar{\sigma}_y\,[\mathrm{nm}]$ | 40/5.5 | 246/19 | 259/2.0 | 300/2.2 | 304/50 | 1587/4 |
| $H_{\mathrm{D}}$ | 3.3 | 2.8 | 1.5 | 1.4 | 4.2 | 1.3 |
| $\bar{\mathcal{L}}\,[10^{33}\,\mathrm{cm}^{-2}\,\mathrm{s}^{-1}]$ | 8.80 | 6.67 | 10.1 | 8.22 | 11.1 | 15.1 |
| $\bar{\mathcal{L}}_1\,[10^{-3}\,\mathrm{nb}^{-1}]$ | 1.30 | 0.76 | 0.74 | 0.51 | 1.39 | 50.2 |
| $\Upsilon_0$ | 0.16 | 0.043 | 0.15 | 0.095 | 0.031 | 0.059 |
| $\Upsilon$ | 0.35 | 0.071 | 0.15 | 0.096 | 0.065 | 0.074 |
| $\delta_{\mathrm{B}}$ | 0.36 | 0.08 | 0.05 | 0.03 | 0.14 | 0.14 |
| $n_\gamma$ | 4.7 | 3.2 | 1.0 | 0.85 | 5.9 | 5.1 |
| $\mathrm{e^+e^-}$ mode | | | | | | |
| $N_{\mathrm{had}}$ | 1.37 | 0.32 | 0.07 | 0.04 | 1.58 | 45.9 |
| $N_{\mathrm{jet5}}\,[10^{-2}]$ | 5.77 | 0.44 | 0.23 | 0.10 | 1.62 | 56.3 |
| $N_{\mathrm{jet10}}\,[10^{-4}]$ | 16.4 | 1.16 | 0.69 | 0.31 | 2.88 | 138 |
| $\gamma\gamma$ mode | | | | | | |
| $N_{\mathrm{had}}$ | 0.15 | 0.10 | 0.19 | 0.14 | 0.13 | 15.2 |
| $N_{\mathrm{jet5}}\,[10^{-2}]$ | 6.90 | 4.72 | 8.61 | 6.43 | 5.68 | 685 |
| $N_{\mathrm{jet10}}\,[10^{-4}]$ | 32.4 | 22.3 | 40.7 | 30.4 | 26.9 | 3240 |

One may on the one hand contrast 'warm' machines with the superconducting TESLA option. Another striking alternative is between CLIC, a two-beam version in which a low-energy, high-intensity drive beam provides the accelerating field for the main one, and all other single-beam designs that will require several thousand klystrons.

Obtaining the required luminosity in a single-pass machine is a real challenge. I adopt as a 'reasonable' goal $L \sim 10^{33}\ (s/(500\ \mathrm{GeV})^2)\ \mathrm{cm}^{-2}\,\mathrm{s}^{-1}$. This represents, per crossing, a gain of 3 orders of magnitude compared to LEP. The key point is to achieve a very small transverse area at the interaction point: the beam size, in particular the vertical one, is now a few to a few tens of nanometres.

A vigorous R&D programme is under way in several places to prove the feasibility of the various options.

*2.3.2 Some facts of life at linear colliders*

Let me present in some detail a few features of the experimentation at a linear collider.

The beamstrahlung parameter $\Upsilon$ measures the effect of the electromagnetic field of a bunch on the particles of the opposite one.

It should actually be computed taking into account the related pinch effect: this gives an effective $\Upsilon$ which differs from the nominal one, $\Upsilon_0$, by as much as a factor of 2 in the case of the relatively small aspect ratio $\sigma_y/\sigma_x$ (i.e. TESLA).

Another key number is $n_\gamma$, the mean number of beamstrahlung photons per electron. Its dependence on the machine parameters is

$$n_\gamma \approx \sigma_z \frac{\Upsilon}{E} = \frac{N/\text{bunch}}{\sigma_x + \sigma_y}$$

exhibiting the linear dependence on $\sigma_z$ for a given $\Upsilon$: having a long bunch has to be paid for.

$\Upsilon$ and $n_\gamma$ are the main parameters governing the electron and photon energy spectra at collision and therefore the differential luminosity curves for ee, e$\gamma$, and $\gamma\gamma$ collisions.

The important features of the curve for $e^+e^-$ are:

- the fraction of the luminosity left close to the nominal value,
- the size of the tail, which may give some beneficial effects ('autoscan') but mostly generates backgrounds.

A very useful fact is that the differential luminosity $L(\sqrt{s})$ can be measured with great accuracy by using the acollinearity of Bhabha events.

Another basic parameter is the intrinsic energy width of the beam (typically 0.1–1%) since it determines the visibility of sharp structures.

Figure 3 shows the photon spectra. The curve marked WW represents the unavoidable Weiszacker–Williams spectrum. The beamstrahlung spectra depend on which version of the machine is considered.

Most important from the experimental point of view are the $\gamma\gamma$ or $\gamma$e interactions at crossing.

Three processes

$$\begin{aligned} \gamma e &\to eee && \text{(Bethe–Heitler)}, \\ \gamma\gamma &\to e^+e^- && \text{(Breit–Wheeler), and} \\ ee &\to eeee && \text{(Landau–Lifshitz)} \end{aligned}$$

give rise to a large flux of soft $e^\pm$. For the modest values of $\Upsilon$ considered, the coherent interactions of a beam particle with the opposite bunch are negligible. The incoherent Bethe–Heitler process is generally dominant. Those of the soft $e^\pm$ that are emitted at large angles or kicked out of the beam by the strong electromagnetic fields will reach the central part of the detector. In spite of the protective effect of the solenoidal field, the flux of $e^\pm$ at the level of an eventual microvertex detector will be very high: care must therefore be taken in the design of this essential detector, and the need for a high fragmentation

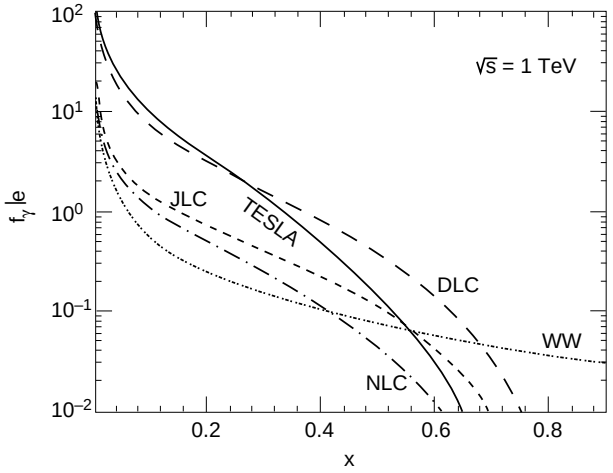


Figure 3: Beamstrahlung spectrum for a TeV collider. The curve labelled WW shows the bremsstrahlung (Weizsacker–Williams) contribution to the photon flux. $x \equiv E_\gamma/E_e$.

will push the use of charge-coupled devices (CCDs) and pixel devices. Although severe, this problem has been shown to be quite manageable.

Most of the pairs created go forward and hit the quadrupoles. Re-emitted soft photons, photoneutrons, etc. are so many that the detector would be swamped by this background: the only way to protect it is by using a shield displayed radially, at a polar angle of $\sim 10°$. At smaller angles there can be no tracking and only rudimentary calorimetry. This 'forward blindness' of a LC detector is an unavoidable feature, the effect of which has to be carefully established for physics.

Another worry concerns the $\gamma\gamma$ hadronic interactions. Photons can interact in different ways: as vector mesons, as partons, or through their quark–gluon content. The uncertainty in the $\gamma$ structure functions led to the conjecture that the rate of hadronic $\gamma\gamma$ interactions leading to minijets could eventually grow quite rapidly with energy. However, the $\gamma$p cross-section measured at HERA and the $\gamma\gamma$ interaction measurements at Tristan have actually excluded the most dramatic rise, although there is still room for some uncertainty. With a well-behaved hadronic-like $\gamma\gamma$ cross-section, the number of underlying $\gamma\gamma$ hadronic events per bunch crossing $[\sim (1 + n_\gamma)^2]$ is generally low, and a fortiori those leading to a substantial jet in the detector. The clarity of LC physics (at least for NLC energies) will not be affected.

It is thus likely that at a LC the most severe background problems will arise from 'trivial' sources: synchrotron, lost particles, muon halo, etc.

*2.3.3 The sunny side: physics prospects*

Figure 4, due to I. Watanabe [7], shows the large variety of channels opened. One can distinguish annihilation channels, decreasing as $1/s$. The $e^+e^- \to Z\gamma$ process is dominant. Most interesting is the $W^+W^-$ final state which gives access to triple-boson couplings. Processes leading to three electroweak bosons are a promise of measuring quartic couplings.

One can also see the rising curves corresponding to fusion processes. In particular one can notice that the Higgs boson production is dominated by fusion above half a TeV c.m. energy.

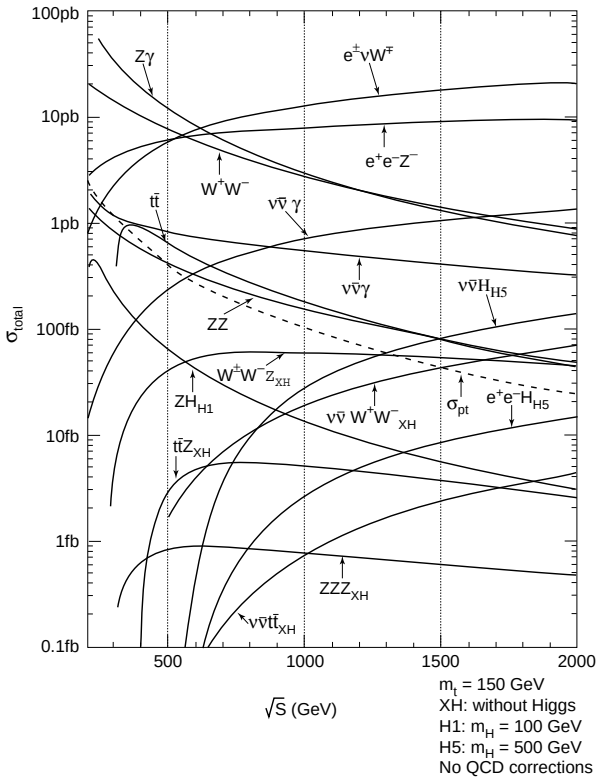


Figure 4: Total cross-sections of the SM processes in the NLC energy region. The figure is due to I. Watanabe. For the cuts required see Ref. [7].

Not shown is the set of $\gamma\gamma$ collision final states whose cross-sections are highly dependent on the $p_t$ acceptance and can reach large values.

*2.3.4 The various modes of a linear collider*

Quite frequently reference is made to c.m. energies and modes of collisions different from the classical $e^+e^-$ NLC.

a) **A Z factory**

No doubt a polarized $Z^0$ factory [7] would bring outstanding physics:

- a new breakthrough in the accuracy of SM measurements, exploitable, as we shall see provided other measurements ($m_{top}$, $e^+e^- \to$ hadrons at low $\sqrt{s}$) are performed as well;
- rare modes of the $Z^0$;
- probably the best place to perform some hot b physics ($B_s^0$ mixing, CP violation in the $B^0$ system, etc.).

b) $e^-e^-$ **mode**

Physics motivations include the desire to reach special quantum numbers, like doubly charged states.

This option requires some thinking about and some R&D since the colliding beams are now mutually defocusing: in particular, it is planned to study what improve-

ments a plasma lens at the interaction can bring, certainly at the expense of an increased background.

c) **A $\gamma\gamma$ collider**

It is, in principle, possible, by backscattering a laser beam on the electron beam just in front of the interaction point, to obtain $\gamma\gamma$ collisions at large $\sqrt{s}$. We shall come back to this option at the end.

d) **Two interaction regions**

Having a single experiment at a LC has always been felt to be a drawback, both from a sociological and a scientific point of view. Actually nothing in principle excludes having two interaction regions, for instance separated laterally: it is, however, clear that the luminosity has to be split between the two experiments, with a time-sharing which can go from a pulse-to-pulse basis to a yearly one.

e) **A TeV collider**

More importantly, as we will see, several plausible scenarios clearly call for a higher c.m. energy than that of the NLC. This should be kept in mind in the conception and R&D programme for the $e^+e^-$ LC of the future. In my opinion, options extendable to higher energies should be considered a first priority.

## 2.4 The LHC

The LHC [8], approved in December 1994, is the pivot of the future of high-energy physics. Much has been said in the lectures of D. Fournier.

Let me briefly present the machine and summarize the physical requirements which motivate the challenging enterprises in the field of detectors described in his lectures.

### *2.4.1 The machine*

The LHC will provide pp collisions with the energy and luminosity needed to obtain parton collisions in the TeV region, at a rate sufficient to exploit the potentially most interesting ones, in particular Higgs boson production.

The LEP machine circumference and the present field limitations of superconducting magnets set a bound to the LHC proton energy: the goal is a c.m. energy of 14 TeV. One is thus led to maximize the luminosity to compensate for this relatively low energy (it was in particular low compared to the design value of the SSC), as one can understand from Fig. 1. The LHC goal is $10^{34}$ cm$^{-2}$ s$^{-1}$: this value, which was recognized as necessary at the time of the 1987 La Thuile meeting, is the real challenge of the LHC both for the machine and the experimentation. To reach it will imply having a bunch crossing every 25 ns and, at each crossing, $\sim$ 20 hadronic interactions will occur. Table 3 shows a few other impressive numbers about LHC, like the stored energy in the beams.

The LHC involves a large set of superconducting magnets. The '2-in-1' solution, in which the two magnetic channels are accommodated in a single structure (Fig. 5), has been adopted, as well as the choice of working at the temperature of superfluid helium (1.8 K). A systematic and beautiful prototyping work has shown that the design field

(8.36 T, for 7 TeV) could be safely reached in such magnets. You can, at CERN, visit an assembly of dipoles and focusing elements, called the String Test, and representing few per mil of the LHC: this will give you a concrete feeling for the size of the enterprise.

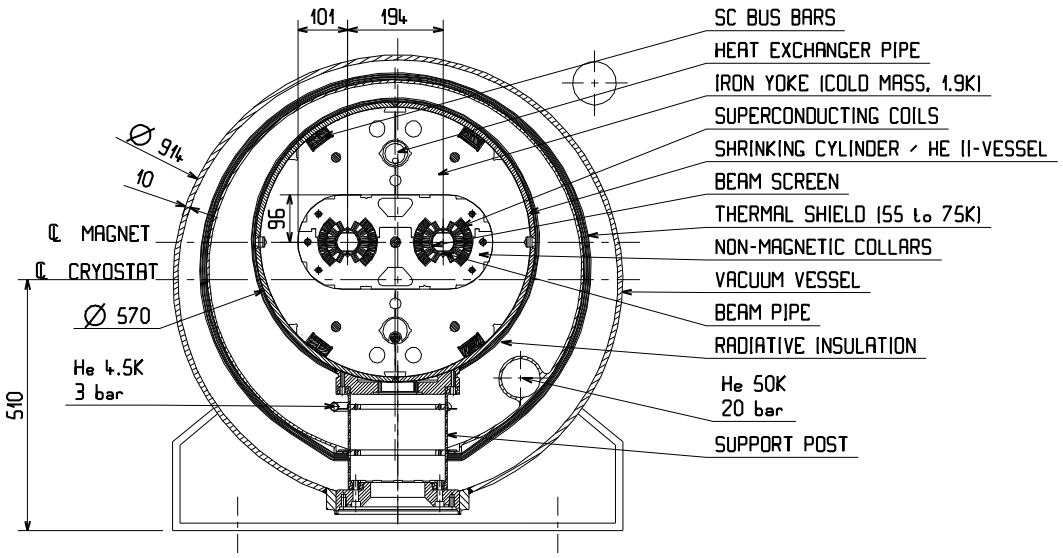


Figure 5: LHC magnet dipole cross-section.

**Table 3:** LHC performance parameters

| | | |
|---|---|---|
| Energy | [TeV] | 7.0 |
| Dipole field | [T] | 8.4 |
| Coil aperture | [mm] | 56 |
| Distance between apertures | [mm] | 194 |
| Luminosity | [$\mathrm{cm^{-2}\ s^{-1}}$] | $10^{34}$ |
| Beam–beam parameter | | 0.0034 |
| Injection energy | [GeV] | 450 |
| Circulating current/beam | [A] | 0.54 |
| Bunch spacing | [ns] | 25 |
| Particles per bunch | | $10^{11}$ |
| Stored beam energy | [MJ] | 334 |
| Normalized transverse emittance | [$\mu$m.rad] | 3.75 |
| r.m.s. bunch length | [m] | 0.075 |
| $\beta$-values at I.P. in collision | [m] | 0.5 |
| Full crossing angle | [$\mu$rad] | 200 |
| Beam lifetime | [h] | 22 |
| Luminosity lifetime | [h] | 10 |
| Energy loss per turn | [keV] | 6.7 |
| Critical photon energy | [eV] | 44.1 |
| Total radiated power per beam | [kW] | 3.6 |

Besides pp collisions, the LHC will offer ion–ion (lead) collisions. The LHC will take the place of the LEP machine in the tunnel, but it is conceivable to install on top of it an optimized electron ring to perform e–p collisions.

The LHC will feed two very large experiments — ATLAS and CMS — providing them with the maximum pp luminosity. Two others — LHCB, devoted to B physics and run at lower luminosity $L \sim 10^{32}$ and the heavy-ion experiment ALICE — are also foreseen (Fig. 6).

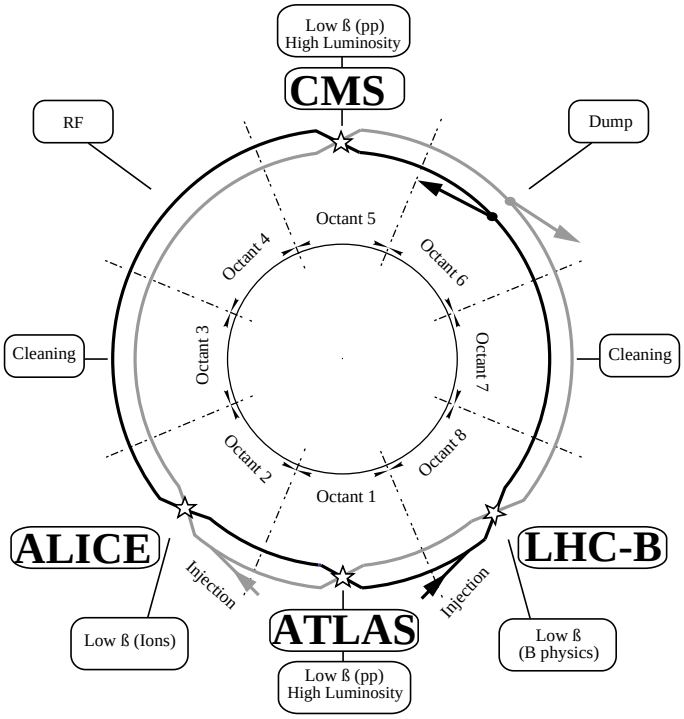


Figure 6: Probable LHC layout with four crossover points.

*2.4.2 The experimentation*

From the experimental point of view the challenge is to cope with this luminosity. As shown by D. Fournier, the high interaction rate will lead to problems of:

- irradiation, up to $\sim$ 100 Mrad/year in the most forward parts, calling for radiation hardness of all components;
- occupancy, up to $10^7$ particles/cm$^2$/s in the central tracking region, calling for extreme granularity and rapidity of the detectors;
- triggering, since the final output of the experiment should not exceed 100 events/s;
- flow of information, with up to 1 MByte of data volume generated by the detector at each crossing.

One may remark that, before the LHC, other experimental programmes [9], like BABAR and BELLE at B factories or HERA B, will already encounter some of these conditions.

These foreseeable problems led to an unprecedented programme of R&D [10], first in the framework of DRD, and now being pursued in the experiments. It will be long and difficult, but very interesting and challenging, and the physics prospects are such that it is being done enthusiastically. For young physicists an ideal situation, in my view,

would be a balanced sharing of activity between an involvement in such preparatory work (instrumentation R&D, preparation of physics, ...) and in an ongoing experiment, so that you get both satisfactions: doing physics today and preparing for tomorrow.

The main lines of physics will be considered in turn. From the detector point of view, the various topics suggest functions to be fulfilled, like detecting leptons, measuring missing $\vec{p}_{\rm t}$, etc. This is summarized in Fig. 7, from F. Pauss. It is essential to see a detector, not only as a juxtaposition of sub-elements, but also from the angle of these 'tasks' which require a close cooperation of several sub-detectors and the definition of procedures.

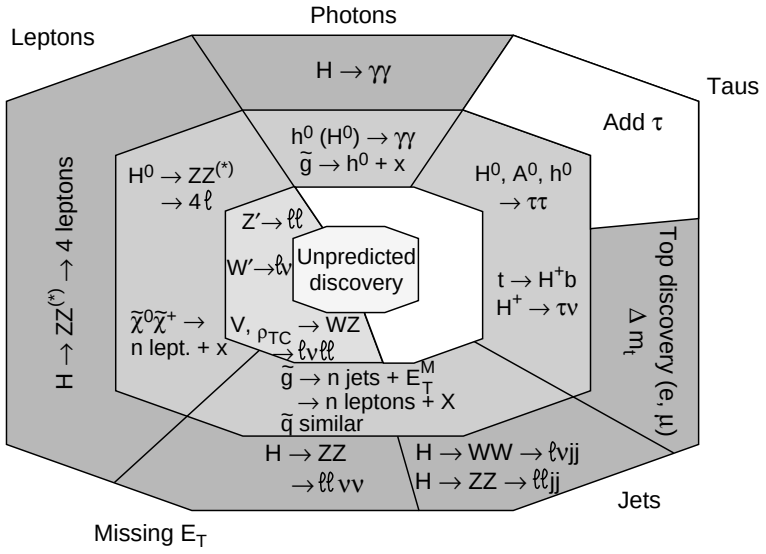


Figure 7: The functions to be fulfilled by the LHC detectors (outer layer) and examples of expected signals. From F. Pauss.

# 3 ACCURATE MEASUREMENTS

## 3.1 Principle of indirect searches

A measurement has to be compared to an expectation. To compute an observable in the SM one needs the input of the three basic electroweak parameters

$$g \qquad g' \qquad v$$

which are actually replaced by the equivalent set of three well-determined quantities

$$\alpha \qquad G_\mu \qquad m_{\rm Z} \ ,$$

the fine structure constant, the muon decay constant, and the $\rm Z^0$ mass, respectively. At tree level, the set ($\alpha$, $G_\mu$, $m_{\rm Z}$) would be enough to compute any leptonic observable. However, the intervention of the SM particles, in particular the top and Higgs, through virtual loop effects, changes the observable value and, in the ignorance of their mass, it is only possible to adopt for it a reference value. For hadronic processes, the strong coupling $\alpha_{\rm s}$ intervenes as well. In summary, for the observable $O$, it is necessary to compute:

$$O(\alpha,\ G_\mu,\ m_{\rm Z},\ m_{\rm top}^{\rm ref},\ m_{\rm Higgs}^{\rm ref},\ \alpha_{\rm s},\ ...)$$

and the goal is to measure an eventual discrepancy:

$$\Delta O(m_{\rm top},\ m_{\rm Higgs},\ ...,\ \text{new physics})\ ,$$

which could be due to a departure of the top and Higgs masses from their reference value, or to new physics. $\Delta O$ should in any case be a small quantity, and this fact calls for the best possible accuracies, both for the experiment and for the theoretical estimate.

Actually the largest virtual effect observed so far is due to the top: up to now accurate measurements at LEP I [11] have essentially been used as indicators of the top mass. The latest combined results from LEP, the SLC and other fields (neutrino scattering, $m_{\rm W}/m_{\rm Z}$) give

$$m_{\rm t} = 178 \pm 8 \pm^{17}_{20}\ \text{GeV}.$$

The central value from LEP alone is $m_{\rm t} = 170$ GeV. The second error is due to the Higgs mass variation, and the lowest value is about that expected in the case of a light Higgs, as in the Minimal Standard Supersymmetric Model (MSSM).

This is in good agreement with the value of $m_{\rm t}$ measured directly at Fermilab

$$m_{\rm t} = 180 \pm 12\ \text{GeV}\ .$$

### 3.2 The best observables

An illustration of the sensitivity of the electroweak observables to various deviations from the SM is given in Ref. [12]. Let us focus on some of the most efficient ones, and introduce useful combinations of them.

*3.2.1* $A_{\rm LR}$

This is the spin asymmetry, obtained simply by comparing the $Z^0$ production cross-section from left- and right-handed $e^-$ in $e^+e^-$ collisions.

Its sensitivity to $\sin^2\theta_{\rm W}$, its low level of detector systematics, and good statistical conditions (all $Z^0$ final states can be used) make it the 'queen' of electroweak observables.

The results come from the SLC and are quite accurate thanks to the high level of polarization. The most recent one interpreted in terms of $A_{\rm e}$ and $\sin^2\theta_{\rm W}$ is:

$$A_{\rm e}\ [A_{\rm LR}] = 0.1637 \pm 0.0075 \quad \sin^2\theta_{\rm W}\ [A_{\rm LR}] = 0.2305 \pm 0.0005\ .$$

In the SM this corresponds to a quite heavy top ($\sim 230$ GeV).

*3.2.2 Other* $Z^0$ *observables from LEP*

Putting together the information from the various asymmetries one gets:

$$\sin^2\theta_{\rm W}\ [\text{LEP}] = 0.23186 \pm 0.00034\ .$$

This is not in good agreement with the SLC value. In particular if one isolates the most accurate single LEP observable, one gets

$$\sin^2\theta_{\rm W}\ [A^{\rm b}_{\rm FB}] = 0.23209 \pm 0.00055\ ,$$

$2.15\sigma$ from the SLC value. Both LEP and the SLC should finally reach an accuracy on $\sin^2\theta_{\rm W}$ of $3\times10^{-4}$. Note that the 'theoretical' uncertainty (see 3.4) is presently $2.3\times10^{-4}$.

*3.2.3* $m_{\mathrm{W}}$

From the hadron collider experiments (CDF and D0 at Fermilab, UA2 at CERN) the present result of the direct measurement is:

$$m_{\mathrm{W}} = 80.26 \pm 0.16 \text{ GeV} .$$

Within the SM frame, one gets from LEP accurate measurements the indirect result:

$$m_{\mathrm{W}} = 80.29 \pm 0.06 \text{ GeV} .$$

Both values agree very well. As in the case of the top mass, within the SM this seems to favour the LEP result on $\sin^2\theta_{\mathrm{W}}$.

The Fermilab Collider will probably reach $\Delta m_{\mathrm{W}} = \pm 100$ MeV or better.

In the LEP 200 Workshops it was shown that by using the reconstruction/rescaling method in the channel $\mathrm{e^+e^-} \rightarrow \mathrm{W^+W^-}$, each of the LEP experiments at LEP 200 should reach for 500 $\mathrm{pb}^{-1}$ an accuracy of $\pm 60$ MeV, largely dominated by statistics. But recent studies claim that the main systematic error in the 4-jet channel ($\sim$ 40 MeV) could actually result from QCD and Bose–Einstein [13] effects leading to 'cross-talk' between the two W's: this deserves further investigation.

The mixed decay channel ($\ell\nu$2J), not affected by such problems, and a measurement at threshold [14] guarantee anyway an excellent accuracy.

Only a LC may, eventually, do better for the $m_{\mathrm{W}}$ measurement, provided systematic errors are well mastered.

### 3.3 The top-mass determination

We quoted above the Fermilab result. Hadron machines will provide the top mass to an accuracy of a few GeV: $\sim 5$ GeV at the upgraded Tevatron, $\sim 3$ GeV at the LHC.

But it will probably be necessary to wait for an $\mathrm{e^+e^-}$ linear collider to get $m_{\mathrm{t}}$ with an accuracy of less than 1 GeV. The behaviour of the $\mathrm{t\bar{t}}$ system near threshold is peculiar and has been well studied. With such a heavy top, no toponium spectroscopy is foreseen. The rise of the $\mathrm{t\bar{t}}$ cross-section at threshold is described by a complicated function, the main variables being $m_{\mathrm{t}}$ and $\alpha_{\mathrm{s}}$, which are strongly correlated. Adding, as a second measurement, the momentum spectrum of the produced top, which has a different correlation pattern, $m_{\mathrm{t}}$ and $\alpha_{\mathrm{s}}$ can be obtained independently, and with great accuracy. Typically, $\Delta m_{\mathrm{t}} = 0.5$ GeV for the range of $m_{\mathrm{t}}$ considered. It is often said that such a step in accuracy for $m_{\mathrm{t}}$ does not help much in the overall testing of the SM. If, for instance, the sensitivity to the Higgs mass is considered, the statement is correct, as long as other measurements stay at the level of accuracy provided by the LEP/SLC era.

### 3.4 The next round of accurate measurements?

However, improvements are foreseeable in the future. A test in depth of the SM is being performed by combining several accurate measurements. Figure 8 [15] shows that the sensitivity to the Higgs mass is optimized by using, for instance, the top-mass measurement, and an excellent determination of $\sin^2\theta_{\mathrm{W}}$. The width of the oblique band corresponds in the figure to $\Delta \sin^2\theta_{\mathrm{W}} = \pm 10^{-4}$, an accuracy three times better than that expected from the LEP/SLC programmes.

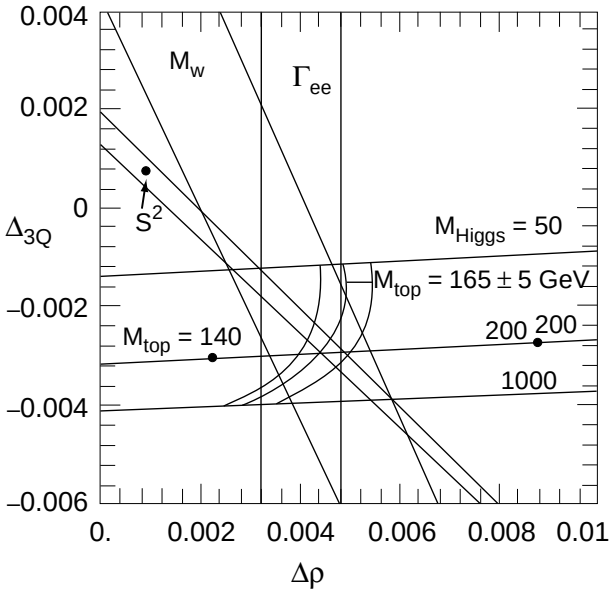


Figure 8: In the plane of variables $\Delta_{3Q}$ and $\Delta\rho$ (see Ref. [15]) the impact of accurate measurements. The oblique band labelled $S^2$ corresponds to $\Delta \sin^2\theta_{\rm W} = 10^{-4}$.

A breakthrough in the accuracy of $\sin^2\theta_{\rm W}$ will require:

i) A much better measurement of $A_{\rm LR}$ on the $Z^0$. This could be obtained if one day high luminosity and large polarization coexist in LEP. It could also come from a polarized $Z^0$ factory, the limit on the precision probably being set there by the limit on the knowledge of the electron polarization.
One may also quote the possibility of measuring $\sin^2\theta_{\rm W}$ at the LHC from the FB asymmetry of the large number of $Z^0$'s produced [16]. While the smallness of the statistical error leaves no doubt, the mastering of systematics at the level quoted has still to be proven.

ii) A more accurate determination of $\alpha(Z^0)$ [17]. It is unfortunate that the extreme accuracy of $\alpha$ at the Thomson limit is of no use for testing the SM: what matters is the precision with which the running of $\alpha$, from $\sqrt{s} = 0$ to $\sqrt{s} = m_{\rm Z}$, is known. This is governed by the knowledge of the vacuum polarization effects, which in turn depend on the quality of the measurement of $e^+e^- \rightarrow$ hadrons between threshold and $\sim$ 10 GeV. We can note that the exploitation of the next round of the $g-2$ experiment is also bound up with such an improvement, but in a region more concentrated near threshold.

If both conditions are satisfied, and $\Delta \sin^2\theta_{\rm W} = 10^{-4}$ is reached, then it is possible to see from Fig. 8 the kind of improvement on the sensitivity to the Higgs mass (considered here merely as an estimator of quality) provided by a better measurement of $m_{\rm t}$.

## 4 DIRECT SEARCHES: THE SCENARIOS

It is not necessary to recall once more the successes of the SM, nor its theoretical shortcomings.

The two main roads beyond the SM are some types of composite scenarios, like technicolour, in which the existence of new types of constituents and interactions is postulated, or the resort to a higher level of symmetry, as in the case of supersymmetry.

In the former case, which seems to meet some difficulties when confronted with the accurate measurements of LEP I [18], one does not foresee the existence of elementary Higgs bosons: one expects instead the appearance at high energy of a new type of strong interaction between the longitudinal part of the intermediate vector bosons. Depending whether this interaction leads to resonance or not, it will be more or less difficult to observe it at the future colliders. In any case it is unlikely that LEP 200 has much to say about this scenario.

The situation is a priori very different if SUSY is the truth. Its rich phenomenology [19] and in particular its very constrained Higgs sector could, as we shall see, already be partly revealed at LEP 200, provided energy and luminosity are sufficient, and at the Tevatron. It would represent a cornucopia for the future large colliders.

It may be useful to spend some time defining which type of supersymmetric theories one is actually considering. The minimal model (MSSM) postulates the minimal set of partners and a Higgs sector made of two doublets, which, after Electroweak Symmetry Breaking (EWSB), amounts to five bosons: the scalars $h^0$ and $H^0$, the pseudoscalar $A^0$ and the charged ones, $H^{\pm}$: its phenomenology will be reviewed below.

SUSY must be broken and this is classically achieved by Soft SUSY Breaking (SSB) terms which avoid the re-introduction of quadratic divergence. In the absence of further restrictive assumptions, the number of such parameters is high. If, however, Grand Unification and gravity-inspired universality are assumed, one is left with the familiar set of five free parameters

$$M,\ m,\ A,\ B,\ \mu\ .$$

$M$ and $m$ are the common gaugino and scalar masses, $A$ and $B$ the trilinear and bilinear couplings of SSB and $\mu$ the Higgsino mixing parameter.

The requirement of a correct EWSB allows one to trade away $B$ and $|\mu|$, while $\mathrm{tg}\,\beta \equiv v_2/v_1$ appears, and one then deals with another usual set:

$$M,\ m,\ A,\ \mathrm{sign}\,(\mu),\ \mathrm{tg}\,\beta\ .$$

Five independent parameters are still a lot and one can further reduce their number and their possible range in different ways.

One way is to impose phenomenological constraints, experimental or cosmological: this leads to various constrained models (CMSSM).

Another way is to get further inspiration on the nature of the soft SUSY breaking terms from Supergravity (SUGRA) and superstrings. This leads to models which, like in the so-called dilaton version of SSB, have finally only two independent parameters [20]. It is fair to say that the corresponding assumptions are far from being proven and one can only consider such models as an interesting and convenient set, in particular to compare the potentials of various machines in exploring the allowed parameter space.

A third possibility, which is linked with the assumed grand unification of b and $\tau$ Yukawa couplings, is the so-called '$m_{\mathrm{top}}$ fixed-point' scenario [21], in which a relation between the top mass and $\mathrm{tg}\,\beta$ is established. With the value found for the mass, one version of this scenario favours a small value for $\mathrm{tg}\,\beta$, between 1 and $\sim 3$. This likely realization of the MSSM will be considered below.

The virtues of SUSY are well known. Quite spectacular is the fact that in SUSY the EWSB is 'built-in', once the top is heavy enough. Figure 9 shows the results of a CMSSM [22], which is only one among several, but nevertheless indicates clearly what

are the strong points on which one should focus first, in particular at LEP 200 and the Tevatron: a general and unavoidable fact is the lightness of $h^0$, the lightest scalar, and this will be quantified in the next section. Another striking fact is that the gauginos, charginos and neutralinos, may be light and within reach, although this is not guaranteed. Another possibility is that, through a large mixing in the stop sector, the lightest stop mass eigenstate is quite low as well.

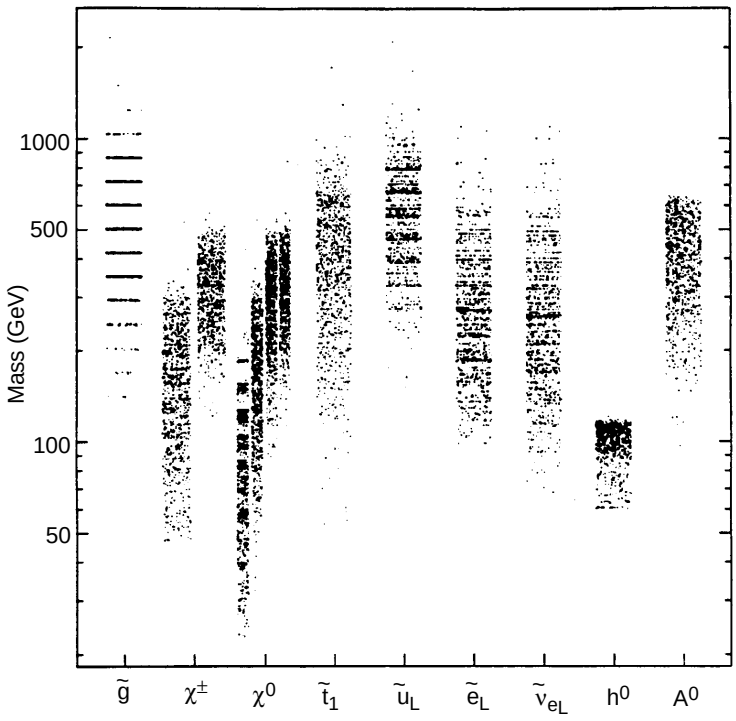


Figure 9: Scatter plot of mass versus particle type in the constrained model of Ref. [22].

## 5 THE HIGGS BOSON(S)

### 5.1 Higgs phenomenology

If, in spite of its shortcomings, one tries to stick to the SM it is natural to study the bounds this model announces for the Higgs mass. In particular, most relevant for LEP 200 is the lower limit that one can deduce from the requirement of stability or metastability of the vacuum [23]. This limit depends on the scale at which the perturbative character of the SM is expected to break down. If the model is supposed to be valid up to the GUT or Planck scale, one finds: $m_{\rm h} \geq 135$ GeV. If, on the contrary, the model breaks down at low energy (1–100 TeV) the limit is lower and the boson could be in the region accessible to LEP 200: however, in such a case, the upper limit is $\sim$ 600 GeV or so, and there is no particular reason to expect the Higgs boson in the 100 GeV region, nor any strong argument to try to gain 10–20 GeV of accessibility there, at any machine.

The situation is totally opposite in the case of SUSY where the lightest boson $h^0$ is bound to exist in this region. The tree-level upper bound on its mass is raised by loop corrections which depend on the fourth power of $m_{\rm t}$ and, logarithmically, on the masses

in the stop sector and therefore on the mixing which determines them

$$m_{\rm h}^2 \leq m_{\rm Z}^2 |\cos 2\beta|^2 + F\left(m_{\rm t}^4, \ln\frac{m_{\tilde{\rm t}}}{m_{\rm t}}, ...\right) \ .$$

In the last few years, the value of $m_{\rm t}$ has been sharpened and the computation of $m_{\rm h}$ in the MSSM has been refined. One can summarize the results by Fig. 10 [24] which shows four extreme cases: large and small tg $\beta$ (i.e. IR fixed point), large and small mixing. It is thus possible to tell which scenarios will be covered by a given mass reach. For instance reaching $m_{\rm h} \cong 110$ GeV would allow one to cover the small tg $\beta$ cases, whatever the mixing, and the large tg $\beta$ case with small mixing, while the large tg $\beta$ situation with large mixing stays partly uncovered.

We recall that, as soon as $m_{\rm A}$ is beyond $\sim$ 100 GeV, the $\rm h^0$ boson is essentially SM-like, both for its bremsstrahlung production mode and in its decay. So the description of the SM boson search which will follow is actually done having the $\rm h^0$ in mind.

A last point is the slow variation of $m_{\rm h}$ in the upper right part of the tg $\beta - m_{\rm A}$ plane: one understands then that a small change in $\sqrt{s}$ can lead to a large one in the coverage of the plane.

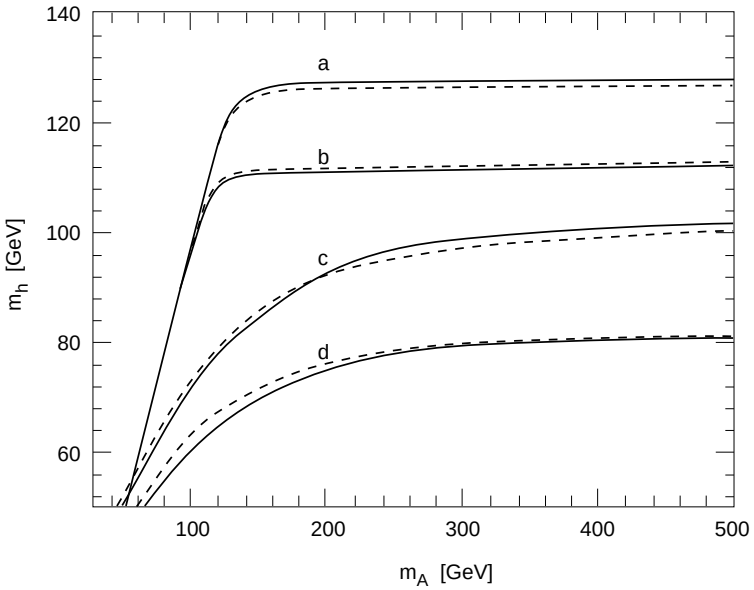


Figure 10: The lightest CP-even Higgs mass as a function of the CP-odd Higgs mass (a) and (b): large tg $\beta$, with large and zero squark mixing, respectively. (c), (d) = small tg $\beta$ (IR fixed point), with large and zero squark mixing, respectively.

## 5.2 Search for the SM Higgs boson

I shall limit myself to a brief status report of the present situation, and a survey of future prospects.

*5.2.1 Production and decay*

The features of Higgs boson production and decay are dominated by its property of coupling preferentially with the highest-mass objects available.

In $e^+e^-$ collisions the SM Higgs production occurs through bremsstrahlung and fusion processes, the latter dominating at high energies. In hadronic collisions, the evolution of gg and qq processes when $m_H/\sqrt{s}$ increases is shown by Fig. 11.

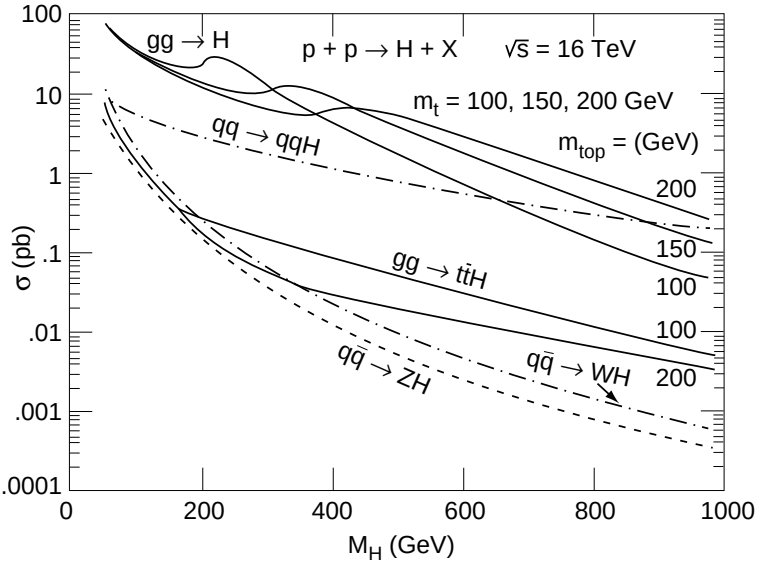


Figure 11: Various components of the Higgs hadronic production cross-section.

The expected decay modes of the SM Higgs boson as a function of its mass are well known: dominance of $b\bar{b}$ up to $\sim 140$ GeV, and then of intermediate boson pairs.

The $2\gamma$ decay mode, vital for the exploration of the intermediate mass region (90–140 GeV) at hadron colliders, occurs through loop diagrams and has a small branching ratio ($\sim 10^{-3}$).

*5.2.2 Higgs search at LEP*

**LEP I**

Searching for a SM-like Higgs boson has been an important activity at LEP I [25].

A low-mass boson was rapidly excluded in all foreseeable decay modes. Focusing on the highest mass region one can, for LEP I, draw the following conclusions:

- the present overall limit is $\sim 65$ GeV;
- one is not far from reaching saturation and only a few GeV more are to be expected;
- while the $H\nu_e\bar{\nu}_e$ channel is still essentially background-free, the $Hl^+l^-$ channel starts being populated and thus weakened by the expected background from four-fermions;
- the 4-jet channel will remain inaccessible for the SM boson search at LEP I in spite of the progress made in b-tagging;
- the alternative mode $e^+e^- \rightarrow H\gamma$ will also stay out of reach in the SM frame. But a level of about $10^{-5}$ for the branching ratio has been reached and this sets limits on various still possible anomalous couplings in the Higgs sector.

**LEP 200**

Figure 12 gives the cross-section of the Higgs production process versus energy and shows that above $m_h \sim 55$ GeV it is more profitable to search for it at LEP 200 [26] than on the $Z^0$ since the cross-section is bigger and the background smaller.

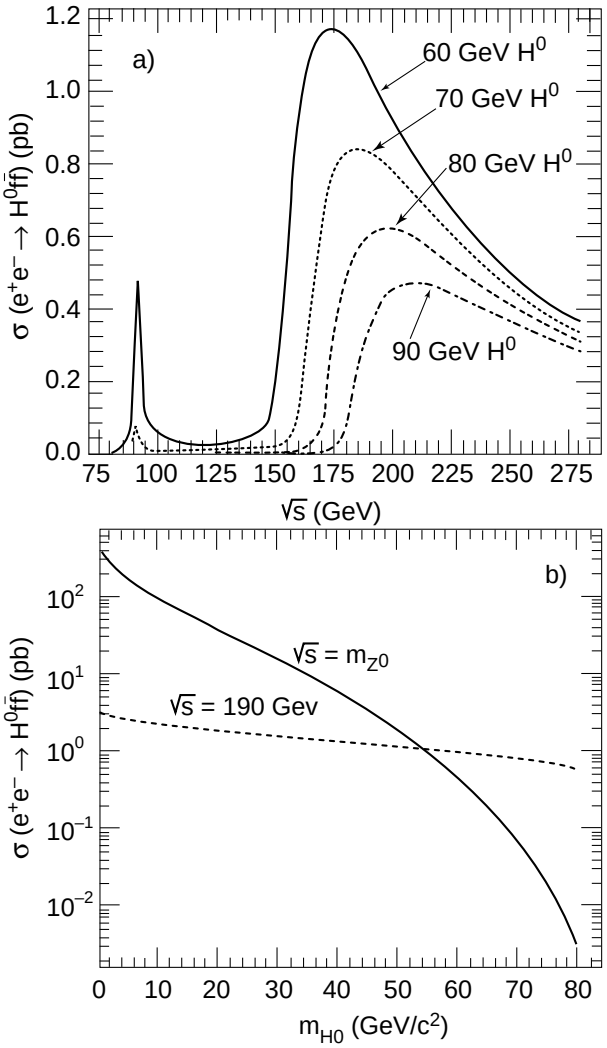


Figure 12: The Higgs boson production cross-section versus $\sqrt{s}$ (a) and versus $m_{\mathrm{H}}$ for two energies (b).

The sharp threshold occurs at $\sim m_{\mathrm{Z}} + m_{\mathrm{h}}$ and one needs $\sim 10$ GeV c.m. more to get close to the maximum of the cross-section: hence the old rule of thumb giving the reach:

$$m_{\mathrm{h}} \sim \sqrt{s} - 100 \text{ GeV} .$$

For the relevant LEP 200 mass region the Higgs boson decays mostly into $\mathrm{b\bar{b}}$ and this explains the overall importance of b-tagging in its search. The $\mathrm{b\bar{b}}$ decay is a tree-level process, unlike the $\gamma\gamma$ mode, and its branching ratio is unambiguously calculable. The $\mathrm{Z}^0$ is observed in the usual ways: $\mathrm{q\bar{q}}$, $\nu\bar{\nu}$ and $l^+l^-$.

Although it is still modest, the fusion channel $\mathrm{e^+e^-} \rightarrow \nu_{\mathrm{e}}\bar{\nu}_{\mathrm{e}}\mathrm{H}$ does exist and interferes with the main one $\mathrm{ee} \rightarrow \mathrm{HZ}(\mathrm{Z} \rightarrow \nu_{\mathrm{e}}\bar{\nu}_{\mathrm{e}})$. This channel is not bound to the kinematical limit expressed above: the possibility that it allows the gain of a few GeV in mass reach is under study.

The background channels are mostly $\mathrm{q\bar{q}}\gamma$ (half being a radiative return to the Z region), WW and ZZ. Combinations of kinematics and b-tagging allow them to be reduced to manageable levels and all HZ modes turn out to be exploitable. The most difficult case

is when $m_{\rm H} \approx m_{\rm Z}$, since the ZZ final state is then kinematically indistinguishable and one rests fully on the b tag.

The b-tag efficiency and purity needed have already been achieved in the present LEP experiments. It was shown that at LEP 200 one can keep $\sim 50\%$ efficiency to the HZ channel and reject WW by $\sim 70$ since there are no b's in W decay.

Even in the most difficult case, the signal/background figures are $\geq 1$. Figure 13 gives for the three energies the exclusion and discovery curves which have the behaviour expected from our previous considerations. To interpret them in terms of running time, one must make tentative assumptions about the experimental procedure at LEP 200: if it is possible to combine the four experiments, as I believe, the luminosity needed per experiment to answer the Higgs question is rather modest and corresponds to at most one year of running.

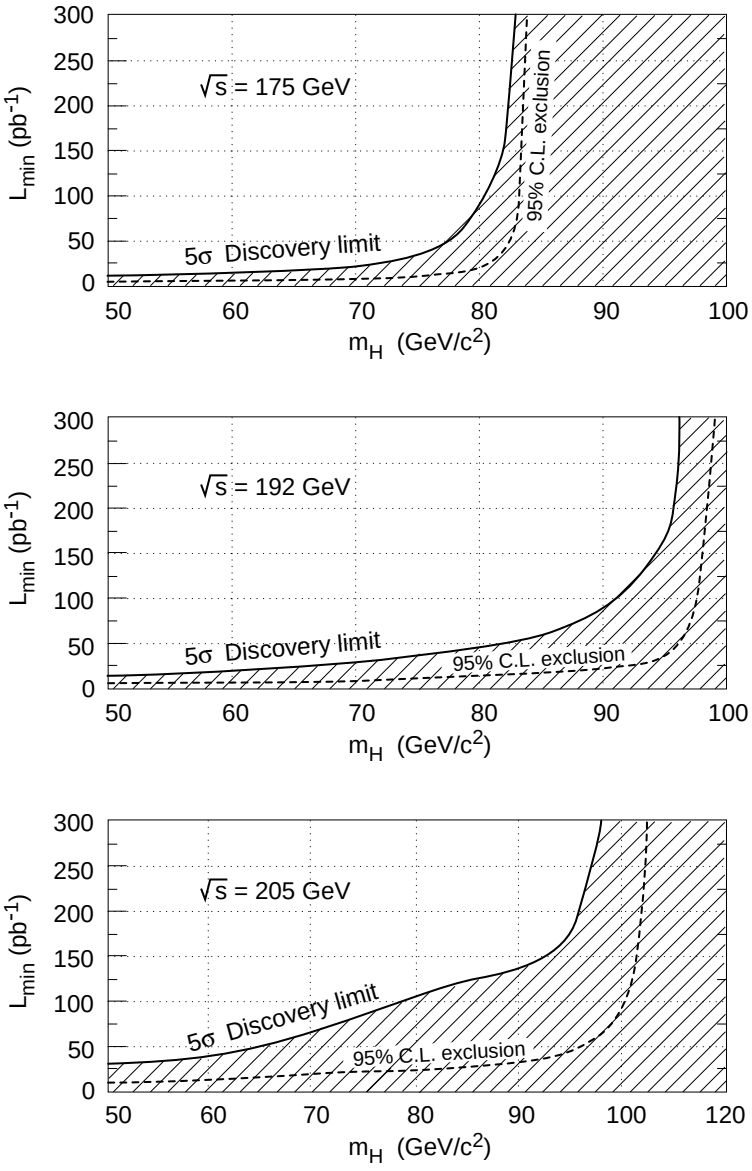


Figure 13: The exclusion and discovery curves for the SM Higgs boson at LEP 200.

The rule of thumb presented above is fairly well verified for discovery: for exclusion at 95% C.L. one still gains $\sim 5$ GeV or so in the mass reach.

On the other hand, the Tevatron, even after its upgrade, would not be able to produce an SM-like Higgs boson in this mass range at a sufficient rate. At least an order of magnitude increase in luminosity — or in the cross-section — would be needed.

### 5.3 Prospects at linear colliders

The problem is quite similar to the one at LEP 200 as long as the bremsstrahlung process dominates: in particular b-tagging will be very useful. It should, however, be remembered that for a given Higgs mass the Higgs cross-section slowly decreases, whilst various fusion backgrounds rapidly increase with $\sqrt{s}$ (Fig. 4): the optimal mode for Higgs study, once it is discovered, is therefore to bring the energy of the machine down to $\sim m_{\rm H} + 110$ GeV.

For $m_{\rm H} \sim 100$–$150$ GeV, at the NLC ($\sqrt{s} \sim 500$ GeV) the fusion mechanism takes over. This machine will allow the discovery of a Higgs boson up to $\sim 350$ GeV, but a 1.5 TeV machine is needed to cover the full mass domain. Various studies [27] have demonstrated that the visibility of a Higgs boson at an LC is guaranteed when the c.m. energy is sufficient.

As previously mentioned, an $e^+e^-$ (or $e^-e^-$) collider can, in principle, be turned into a $\gamma\gamma$ collider: this would be an ideal machine to study (but not to discover) the Higgs boson as we shall see below.

### 5.4 Prospects at the LHC

Future large hadron colliders have a large potential for the exploration of the Higgs sector [28].

The production cross-section shown in Fig. 12 is relatively comfortable up to $m_{\rm H} \sim 800$ GeV.

When the Higgs boson decays substantially into a pair of Z's and is abundantly produced, namely for $140 \lesssim m_{\rm H} \lesssim 800$ GeV, the search, through four-lepton final states, is relatively straightforward.

On the other hand, the extreme regions below $\sim 140$ GeV (a) and above $\sim 800$ GeV (b) are certainly quite difficult to explore.

In (a) one way is to rely on the $H \to \gamma\gamma$ mode in spite of its small branching ratio. With an outstanding electromagnetic calorimeter, retaining its quality at full luminosity, the signal should be visible over the irreducible $2\gamma$ background spectrum: this assumes that the reducible background from $\pi^0$'s or jets mimicking a photon, can be mastered, as well as the background from $Z^0 \to e^+e^-$, with the e confused with a $\gamma$, for masses around 90 GeV.

The possibility to observe the light Higgs boson in its dominant $b\bar{b}$ decay mode, when it is tagged by the presence of a W or a $t\bar{t}$ system, is considered as well, after the encouraging results of b identification by the CDF microvertex.

Above $\sim 800$ GeV, various tricks such as those described in the case of a strongly interacting sector (central jet veto, forward jet tag) have to be used.

If reality conforms with Monte Carlo expectations, the hadron colliders, with several years at full luminosity, should solve the SM Higgs problem.

## 5.5 The MSSM Higgses

The previous section devoted to the SM Higgs describes as well the search for $h^0$ through the bremsstrahlung mechanism. However, in the case of SUSY, one can also exploit the Associated Production (AP) processes.

### *5.5.1 LEP 200*

The relevant AP process is there: $e^+e^- \to A^0h^0$ [26].

The complementarity between the two mechanism is well known, although the P wave AP has the handicap of a (velocity)$^3$ factor. At large $\mathrm{tg}\,\beta$ and modest $m_A$, the AP dominates, while it is the contrary at small $\mathrm{tg}\,\beta$.

The AP process, leading to 4 b's, is particularly prone to b-tagging: this is welcome to allow the elimination of the much larger WW background, which is kinetically identical to the signal when $m_A \sim m_h \sim m_W$.

Let us recall that at LEP I both h and A are excluded up to 45 GeV. Searches for hA associated production in the 4b final state exploiting b-tagging were particularly efficient.

However, this result is obtained for a particular set of SUSY parameters corresponding to no or small mixing in the stop sector.

Turning now to the prospects for LEP 200, the exclusion/discovery domains in the $\mathrm{tg}\,\beta - m_A$ plot are shown in Fig. 14. One distinguishes clearly the regions where the two search channels dominate. The coverage obtained through the bremsstrahlung channel depends critically, as we saw previously, on the available $\sqrt{s}$, and also, for a given $m_{\mathrm{top}}$, on the level of mixing in the stop sector.

At $\sqrt{s} = 205$ GeV, small mixing and $1\,\mathrm{fb}^{-1}$, the plane is nearly fully covered. This can be seen also in an alternative representation using the $(m_h, \mathrm{tg}\,\beta)$ plane.

One must remember that, in particular in the case of SUSY, one may be led to a situation where the Higgs bosons decay invisibly. This can happen if the $\chi^0\chi^0$ decay mode is open, or in various scenarios of R parity breaking.

Detecting this mode is possible at $e^+e^-$ machines.

### *5.5.2 LHC*

Here again the c.m. energy opens a large set of possibilities, described in the now familiar MSSM plot $\mathrm{tg}\,\beta - m_A$. To simplify the presentation, let us consider separately the various channels. The LHC potential is summarized by Figs. 15(a)–15(d).

One will search, as in the SM case, for a signal in the $\gamma\gamma$ mode. For SM-like couplings the reach is given by Fig. 15(a). The two large experiments are rather equivalent, and the apparent difference of coverage reflects the different assumptions made. A caveat: since both h production and $h \to \gamma\gamma$ decay are mediated by loops, one should in principle take into account the actual population of particles circulating in the loops, which depends on the actual SUSY scenario.

Another direct signal to be searched for is the 4-lepton one [Fig. 15(c)], which allows the coverage of the bottom region of the diagram. One may notice here that such a channel would reveal the existence of the H boson, while in the same region LEP 200 would give access to the h boson: this illustrates the complementarity between the information of different machines.

Other channels, like $\tau\tau$ or $\mu\mu$, can reveal the existence of Higgs bosons in different regions of the MSSM plane, above the lines shown in Fig. 15(b) and 15(d).

Putting together the various pieces of information one will essentially cover all the plane, with the possible exception of a 'hole' around $m_{\rm A} \sim$ 100–200 GeV, tg $\beta \sim$ 5–10. The size of the hole depends on the luminosity considered and on the actual physical parameters. For instance, a heavier top is favourable to the LHC potential of exploration (and unfavourable to the LEP 200 one as we noticed).

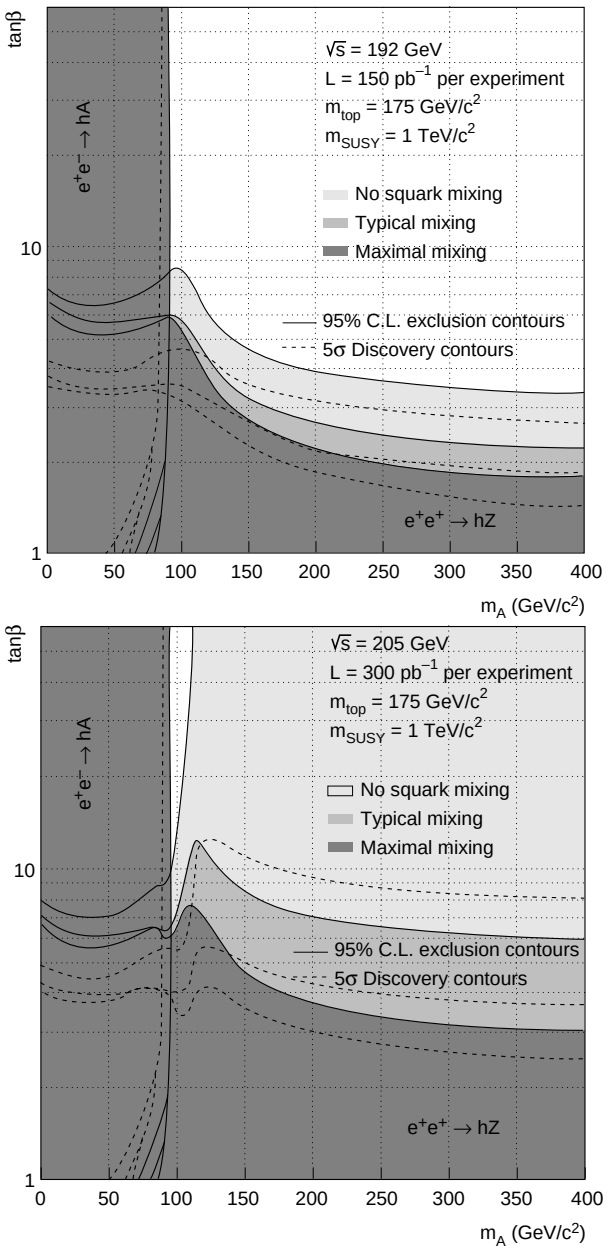


Figure 14: The exclusion/discovery domains in the tg $\beta - m_{\rm A}$ plot at LEP 200 for two energies and various sets of parameters.

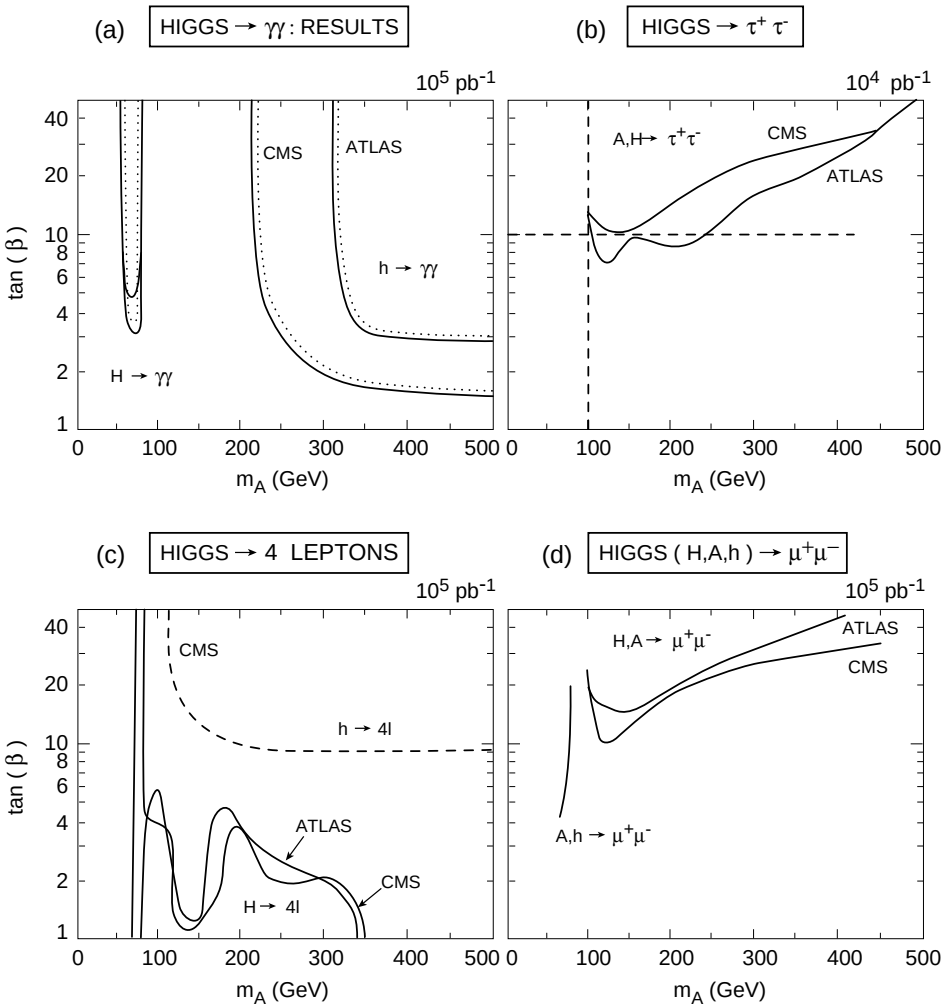


Figure 15: The discovery contours in the $\mathrm{tg}\beta - m_{\mathrm{A}}$ plot at the LHC for four decay modes of Higgs bosons.

*5.5.3 Linear colliders*

It is likely that a LC will be built after the bulk of the exploratory work by the LHC.

Here again the potential is large and the visibility of Higgses is guaranteed.

One can probably say that the roles of a LC will be:

1) To complement the exploratory work, in particular for special cases, like invisible modes of boson decay, which may be difficult to deal with at the LHC. Experience and simulation show that their observation should not be a problem at $e^+e^-$ machines.

2) To distinguish between scenarios, in case of discovery, and to bring quantitative information.

   The first goal, if a single boson has been discovered by then, would be to decide whether one is dealing with SUSY or not by getting evidence for eventual partners, and/or by measuring its branching ratios with enough accuracy to draw conclusions [29]. This is illustrated by Fig. 16 [27] which shows the domain in which such conclusions can be drawn.

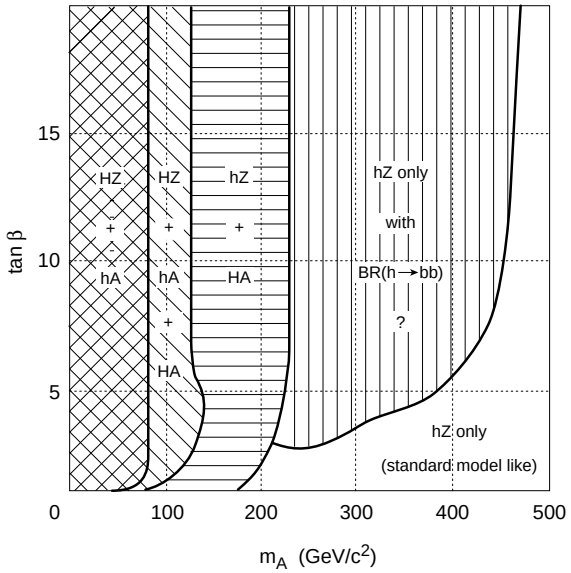


Figure 16: Regions of the tg $\beta - m_{\rm A}$ plot for which LEP 200 and a Linear Collider can distinguish SUSY from the SM.

# 6 OTHER SEARCHES

## 6.1 Generalities

The first role of new machines is to perform a general exploration for new particles or mechanisms, with as few biases as possible about what they could be. As said earlier, this should lead to putting the accent on topologies rather than on specific fully defined channels.

For the discovery potential, it is clear that the LHC, because of its c.m. energy, luminosity, and broadband beams of partons, has no rival, provided the final state is striking enough to stand out clearly above background. Recurrences of electroweak bosons, decaying into lepton pairs, are a good example (Fig. 17).

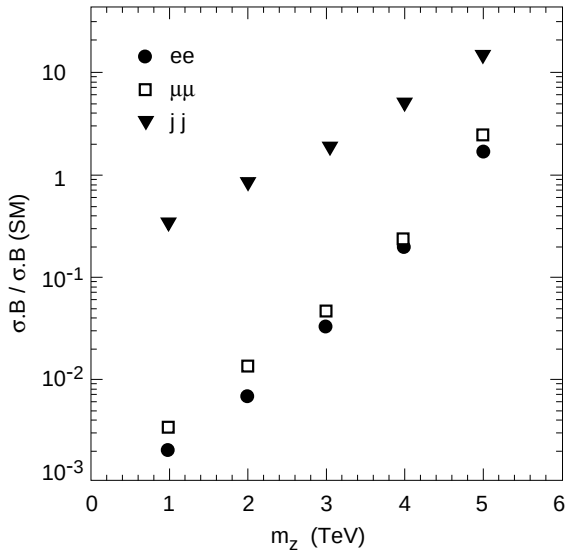


Figure 17: Discovery mass limits for a Z′ ($10^5\,{\rm pb}^{-1}$).

One usually considers an $e^+e^-$ collider as a measurement rather than as an exploratory machine. This is only partly true, and an equally founded statement could be that hadron machines are best-suited to deal with strongly interacting particles and $e^+e^-$ machines with weakly interacting ones. Let us illustrate this point of view and possible exceptions in the case of a few SUSY spartners.

## 6.2 Strongly interacting particles at hadron colliders

Proton machines are indeed the right ones to look for squarks and gluinos. The production rates are sufficient up to very large masses (15 to 20% of the c.m. energy, typically) and depend actually on the $\tilde{g}/\tilde{q}$ mass ratio. The decays are cascades through gauginos and the fraction of missing energy depends on the detail of the cascade, the shortest one (i.e. direct decay to LSP) giving the best signature through missing energy. Another possibility is to look for multileptons issued from gaugino decays. In particular same-sign dileptons can stem from both gluinos decaying to charginos, because gluinos are Majorana particles.

Present limits of Fermilab are reaching typically 200 GeV. The prospect at the upgraded collider is to gain still a factor $\sim 1.5$. As for the LHC the reach is quite impressive as shown by Fig. 18. Actually, even with a lower initial luminosity, a large exploration of this sector can be made rapidly.

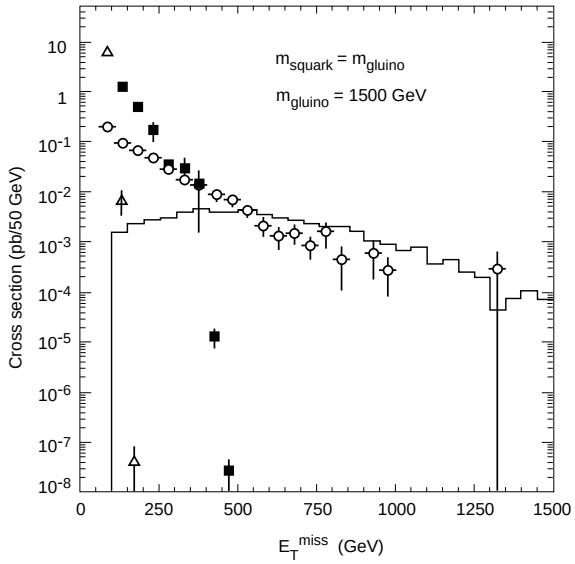


Figure 18: Cross-section as a function of $E_{\mathrm{T}}^{\mathrm{miss}}$ for $m_{\tilde{q}} = m_{\tilde{g}} = 1500$ GeV (full line) and for various backgrounds (from ATLAS Technical Proposal for explanations).

## 6.3 Weakly interacting particles at $e^+e^-$ machines

*6.3.1 Gauginos*

For charginos the situation was very simple at LEP I where the only production diagram is $Z/\gamma$ exchange: the scan allowed one to set a limit on its mass of 47 GeV, provided that the lightest neutralino is below 41 GeV.

At LEP 200 the $\tilde{\nu}_e$ t-exchange amplitude can interfere destructively with the previous one, and some set of parameters, with small $m_{\tilde{\nu}_e}$, may in principle lead to small cross-sections.

A systematic scan of the MSSM parameters was performed and the result is shown in Fig. 19 [26]. Only a small fraction of pathological cases correspond to a cross-section below $\sim$ 1 pb at LEP 200. One should add the condition that the chargino mass be at least 5–10 GeV above the LSP one, so that visibility is guaranteed. The conclusion is that most of the possible cases lead to a clearly observable situation, where chargino discovery, through a set of kinematical cuts rejecting WW background, is achievable with the luminosity foreseen.

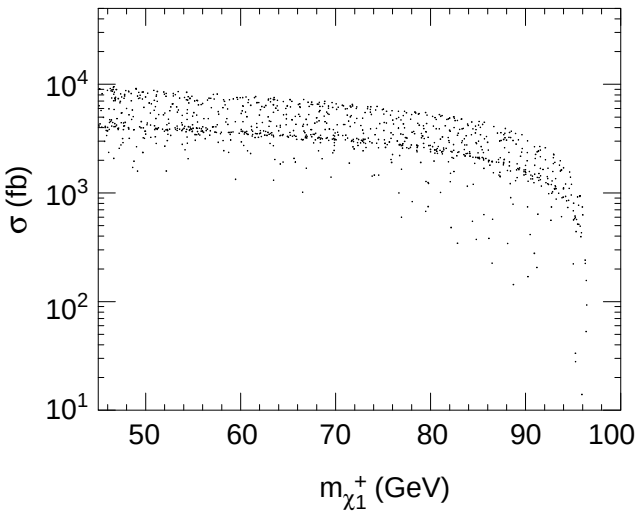


Figure 19: Charginos at LEP 200: result of a scan of SUSY parameters (Ref [26]).

Could neutralinos add some relevant information?

At LEP I the $Z \to \chi_i \chi_j$ coupling in the MSSM is large if $\chi_i$ and $\chi_j$ are higgsino-like, vanishing if $\chi_i$ or $\chi_j$ are pure gaugino. The Z line shape measurement rapidly allowed the exclusion of a large region of the parameter space. But even direct searches for $Z \to \chi^0 \chi'^0$ (since $\chi^0 \chi^0$ is not accessible) are not sufficient at small tg $\beta$: for tg $\beta < 2$ one does not get a limit on the $\chi^0$ mass. One must then invoke the gluino mass limit of hadron colliders as a substitute.

At LEP 200 the neutralino search may allow the coverage of small regions of the $M$, $\mu$ parameter space which are not kinematically accessible through charginos, provided other parameters are such that the rates are large enough.

What about the potential impact of the Tevatron for gaugino searches? The cleanest observable there is the three-lepton final state from $\chi^0 \chi^{\pm}$ associated production. The present mass reach quoted is slightly above the LEP one and it will rise rapidly with increased statistics. But, as shown in Fig. 20 [26] which represents a scan of parameters, the situation is very model-dependent: with the $fb^{-1}$ foreseen at the upgraded Tevatron one can reach mass values as high as 150 GeV, with a reasonable probability of discovery, but in case of a negative result it will be impossible to set a lower limit.

In the particular frame of SUGRA and string-inspired models one can make a similar comparison of the potential of LEP 200 and the Tevatron: the competition between them is quite manifest.

Any increase in LEP energy above the $Z^0$ will improve the mass reach for the charginos and, until the W pair threshold is crossed, a very modest exposure is sufficient to conclude. This has just been achieved, at the time of writing, for $\sqrt{s} = 130$ and

136 GeV. The conclusion is that the chargino is heavier than 65–68 GeV, depending on its content and the mass difference with the LSP.

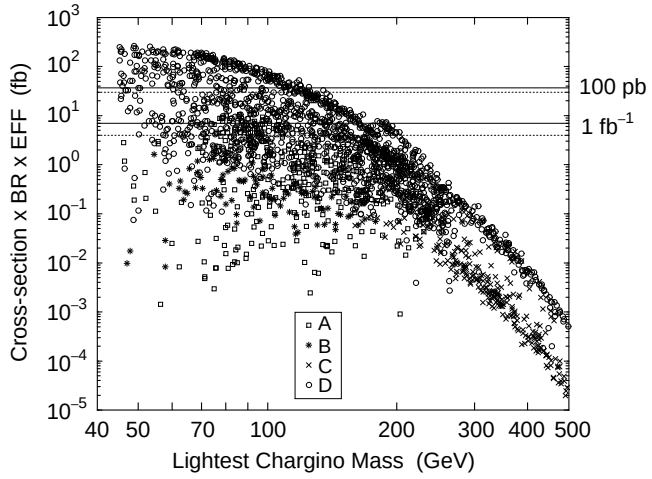


Figure 20: Charginos at the Tevatron: result of a scan of SUSY parameters (Ref. [26]).

*6.3.2 Gauginos at linear colliders*

A linear collider could benefit from its luminosity and clean conditions to perform some metrology in the field of gauginos, like their mass determination.

This is illustrated by Fig. 21 [30].

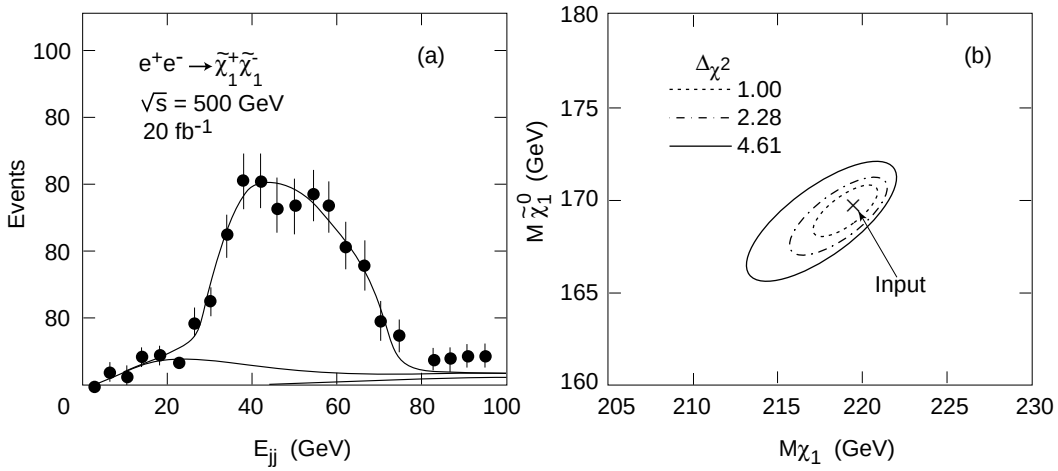


Figure 21: Determination of the chargino and LSP masses at a LC (see Ref. [30]).

*6.3.3 Sfermions*

Although there is no compelling argument, it may be that sfermions, in particular the $\ell_R$ spartner, are light. This can occur in some of the models alluded to in Ref. [20].

This is especially true for the stop: owing to the large top mass, mixing between states could be important and the lightest resulting one be very light indeed.

Through its decay to $c\chi^0$ through a loop, or eventually the tree level decay $b\chi^+$ if kinematically accessible, the stop can be found at $e^+e^-$ machines.

However, the Tevatron also has a large discovery potential for the stop, through $c\chi^\circ$ and $b\chi^\pm$ final states: here again the machines are in competition.

The recent high-energy run of LEP has set limits at $> 57$ GeV ('left' component) and $> 48$ GeV ('right' component).

## 7 WW COUPLINGS

The SM predicts a definite form for the multiboson couplings [31]: this part of the SM has, however, never been checked directly. The channel $e^+e^- \to W^+W^-$ is the right one to do so. The properties to be demonstrated are summarized by Fig. 22.

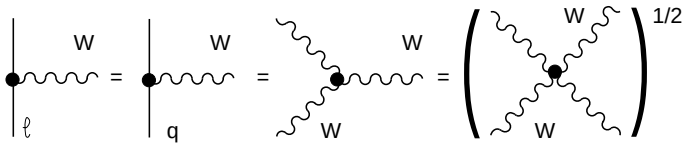


Figure 22: A diagrammatic expression of the SM predictions for electroweak boson couplings (from K. Hagiwara).

In full generality five independent anomalous couplings should be introduced (we assume CP conservation); they are related to eventual W anomalous properties. Further theoretical assumptions lead to relationships between these anomalous couplings and allow the number of free parameters to be decreased. By simple arguments one can understand that the sensitivity to a given anomaly increases with c.m. energy.

Detailed studies have shown that LEP 200 [32], provided that the planned energy and luminosity are reached, will set limits on anomalous couplings at the level of

$$\Delta g \sim 0.1$$

where $g$ is used here as a generic name for an anomaly.

Similar studies were done for LC. At the NLC it seems that $\Delta g \sim 0.01$ can be obtained. Furthermore, an increase of $\sqrt{s}$ allows the accuracy to be improved: 1 TeV could push it to a few per mil.

Hadron colliders cannot use the $W^+W^-$ channel, swamped by background, but can get equivalent information from WZ and $W\gamma$ channels. A sensitivity of $\sim 0.01$ can also probably be obtained.

Figure 23 gives an overview of the potential reach of various machines. The key question is to know what is the expected size of such effects. Estimates range between a few per cent and a few per mil, although no firm arguments can be put forward. A safe objective could be to reach the level of the expected electroweak radiative corrections amounting to a few per mil.

The argument [33] according to which low-energy (LEP I, etc.) measurements already preclude the existence of anomalies may be valid for the LEP 200 case, with possible exceptions, but is certainly irrelevant for the level of accuracy we are discussing here.

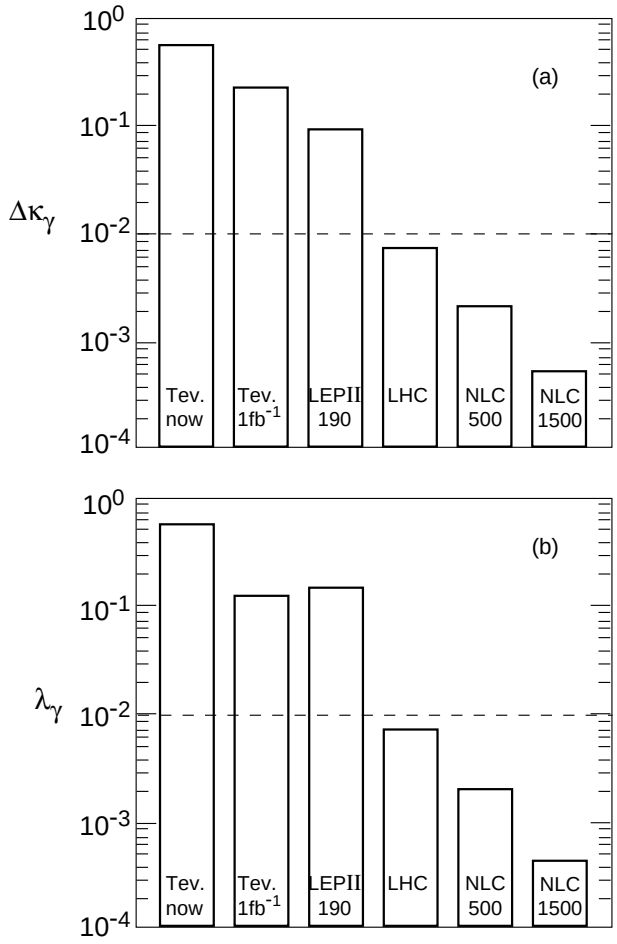


Figure 23: The expected accuracy on anomalous couplings at various machines.

## 8 STRONGLY INTERACTING SECTOR

An experimentally related topic is the study of scenarios, mentioned in Ref. [34], where a strong interaction of electroweak vector bosons — more exactly of their longitudinal part — appears at high energy.

This new interaction may be resonant or not. Its manifestation replaces the usual Higgs phenomenology.

In brief, at $s \gg m_{\mathrm{W}}^2$, the W longitudinal polarization vector is $\epsilon_{\mathrm{L}}^{\mu} \approx (p^{\mu}/m_{\mathrm{W}})$, leading for $\mathrm{W_L W_L}$ scattering to amplitude $\sim s/v^2$ ($v$ is defined in 3.1).

In the SM the Higgs boson helps, by replacing $s$ by $m_{\mathrm{H}}^2$. However, if there is no Higgs boson below $\sim 800$ GeV, $\mathrm{W_L W_L}$ scattering becomes strong anyway.

So one must study this channel and more generally longitudinal boson-pair scattering.

As an example of resonant interaction one can consider technicolour (although we know that present accurate electroweak measurements give a hard time to such theories) and the case of '$\rho$-like' resonance ($I = J = 1$) or techni-$\rho$.

In the $\mathrm{e^+e^-} \to \mathrm{W_L W_L}$ process the techni-$\rho$ acts as a rescattering coefficient $F_{\mathrm{T}}$: experimentally the goal is, through a full angular analysis of the final state, to determine Im $F_{\mathrm{T}}$ and Re $F_{\mathrm{T}}$.

The likelihood contours obtained from a Monte Carlo study for the L.C. c.m. energy and integrated luminosity quoted are shown in Fig. 24 [35] for a techni-$\rho$ of 1.7 TeV. One sees that even with generous exposures one needs to go beyond $\sqrt{s} = 500$ GeV to get clear evidence for the phenomenon.

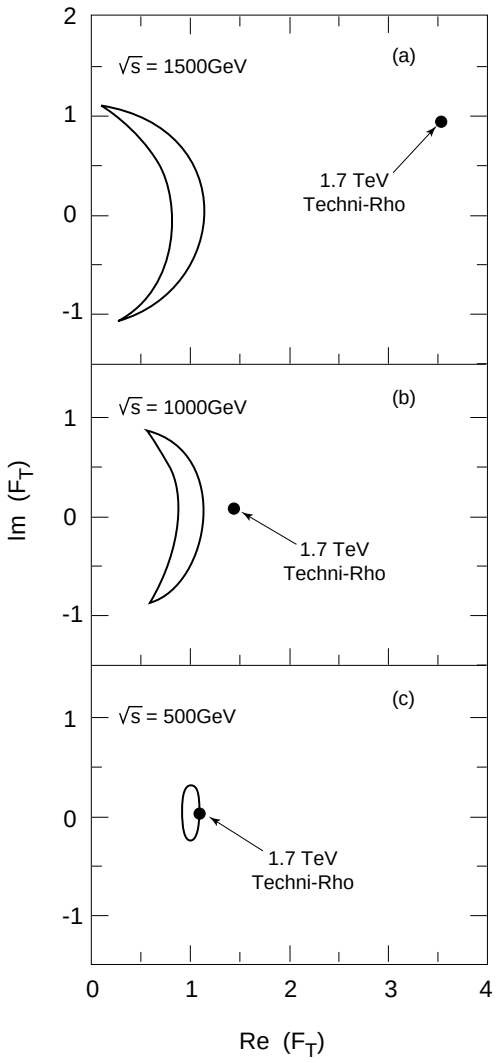


Figure 24: Im $F_{\rm T}$ versus Re $F_{\rm T}$ for a 1.7 TeV techni-$\rho$. The 'moon' around the SM point (0,1) is the sensitivity limit.

Such scenarios (see also the BESS model [36]), as in the case of a heavy Higgs, are incentives to consider machines beyond the NLC.

At the LHC a variety of resonant scenarios should be clearly identified in the leptonic channels (Fig. 25). Non-resonant ones may appear in different versions: one keeps the guidance of low-energy theorems (LETs) with various ways of implementing unitarity. Here the situation may be quite difficult. One will use observables built from gold-plated leptonic decays of boson pairs, with various tricks (tag of forward jets, ...) to enhance the signal over background as shown by Fig. 26 from ATLAS. It is clear that owing to the very low rate and the absence of distinct shape of the signal, which requires then a good knowledge of the absolute efficiency, the observability of such unfavourable scenarios is a real challenge.

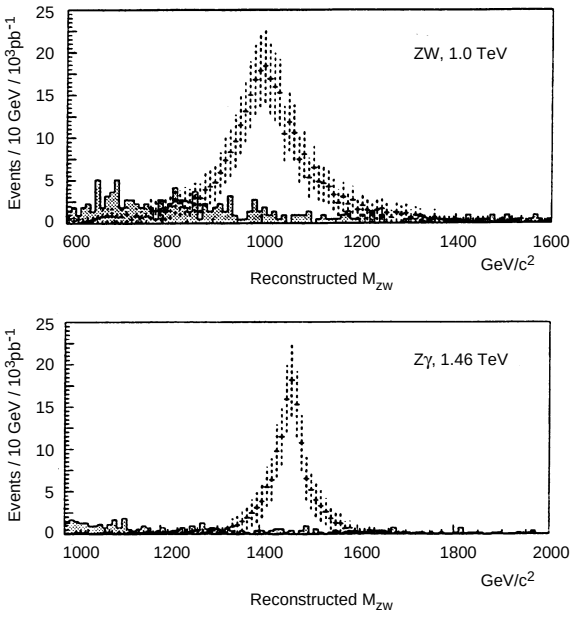


Figure 25: Visibility of technicolour resonances at LHC (from ATLAS).

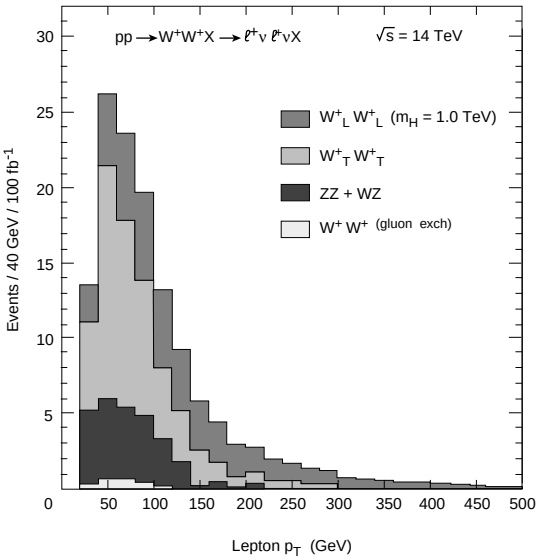


Figure 26: The lepton $p_{\mathrm{T}}$ spectrum from $\mathrm{W^+W^+}$ in the case of a very heavy Higgs (or a strongly interacting scenario) (from ATLAS).

## 9 ... AND FUN FOR THE END

Since you are young people and have plenty of time ahead of you, let me present briefly two futuristic machines.

### 9.1 A $\gamma\gamma$ collider

By backscattering a laser on an electron beam one can get very energetic photons, at an angle $\sim 1/\gamma$ (i.e. microradians in our case) from the beam. Doing that on both sides at the final focus of an $e^+e^-$ (or $e^-e^-$) collider, one obtains then $\gamma\gamma$ collisions at a c.m. energy comparable to the one of the collider [37]. An intermediate step would be to perform $e\gamma$ collisions.

Table 4 (from V. Balakin) shows the parameters of a relatively low-energy $\gamma\gamma$ machine ('Higgs factory'). The luminosity can be potentially very high since the interacting beams are neutral. However, the last-but-one line already gives an idea of the problem: the beam–laser interaction for the parameters given should occur not more than half a millimetre away from the interaction point, otherwise the natural $1/\gamma$ 'opening' blows up the transverse area and kills the luminosity.

**Table 4:** Parameters of a $\gamma\gamma$ Higgs factory (from V. Balakin)

| | |
|---|---|
| Electron energy [GeV] | $2 \times 120$ |
| Photon energy [GeV] | $2 \times 100$ |
| Luminosity $\gamma\gamma$ [$\mathrm{cm}^{-2}\,\mathrm{s}^{-1}$] | $5 \times 10^{35}$ |
| Length [km] | $2 \times 1.7$ |
| Repetition rate [Hz] | 900 |
| Linac wavelength [cm] | 4.2 |
| Number of electrons | $4 \times 10^{11}$ |
| Bunch sizes $\sigma_z$ [mm] | 0.75 |
| $\sigma_x$ [$\mu$m] | 0.2 |
| $\sigma_y$ [$\mu$m] | 0.0038 |
| Beta functions $\beta_x$ [mm] | 0.7 |
| $\beta_y$ [mm] | 0.35 |
| Emittances $\gamma\epsilon_x$ [m rad] | $2 \times 10^{-3}$ |
| $\gamma\epsilon_y$ [m rad] | $0.7 \times 10^{-8}$ |
| BNS parameter $\sigma_E$ [%] | 3.5 |
| Conversion coefficient | 0.7 |
| Conv. –I.P. distance [mm] | 0.5 |
| Quantum parameter $\langle\Upsilon\rangle$ | 0.6 |

I do not think anyone has produced a realistic scheme, nor a suitable laser, up to now. See, however, Ref. [38] for guidance. Nevertheless it is worth pursuing (with maybe a less ambitious initial goal than in Table 4) since $\gamma\gamma$ collisions would provide final states with an original set of quantum numbers. In particular the Higgs boson would be produced in the $s$-channel, through a loop diagram in which all existing heavy particles 'circulate'.

Furthermore, by proper manipulation of helicities (i.e. electron beam and laser polarization) one can, in principle, provide a rather monochromatic luminosity spectrum, so that, assuming the boson has been discovered somewhere else, one can set the machine at the right energy to concentrate the luminosity at its mass, thus optimizing the signal/background ratio.

### 9.2 A muon collider

Compared to electrons, muons have two main advantages due to their mass: they do not radiate much, and, in the case of a mass-dependent coupling like to the Higgs, they are much more strongly coupled. Unfortunately they are unstable and will only make a few turns in a storage ring: this number actually only depends on the guiding field value:

$$N_{\rm turns} = 300 \times B\,({\rm Tesla})\ .$$

One has to produce muons, cool them, accelerate them, and store them. The first step, given the luminosity required, is probably the most difficult since one needs a very fast cycling, very high intensity proton machine, as indicated in Table 5. Cooling can use original methods, like $\mathrm{d}E/\mathrm{d}x$ cooling, because of the depth of penetration of muons. One then needs a high-energy linac and a storage ring.

This bold idea is generating much interest at the moment [39].

**Table 5:** Parameters of possible muon colliders

| Parameter | Symbol | High-energy | Higgs factory |
|---|---|---|---|
| Energy per beam | $E_\mu$ | 2 TeV | 100 GeV |
| Luminosity | $L = f_0 n_{\rm s} n_{\rm b} N_\mu^2 / 4\pi\sigma^2$ | $5 \times 10^{33}\,{\rm cm}^{-1}\,{\rm s}^{-1}$ | $4 \times 10^{29}\,{\rm cm}^{-1}\,{\rm s}^{-1}$ |
| HEH-source parameters | | | |
| Proton energy | $E_{\rm p}$ | 40 GeV | 40 GeV |
| Protons/pulse | $N_{\rm p}$ | $2 \times 10^{14}$ | $10^{14}$ |
| Pulse rate | $f_0$ | 30 Hz | 10 Hz |
| $\mu$ production efficiency | $\mu/p$ | $2 \times 10^{-3}$ | $10^{-3}$ |
| Collider parameters | | | |
| Number of $\mu^+/\mu^-$ per bunch | $N_{\mu\pm}$ | $2 \times 10^{11}$ | $2.5 \times 10^{10}$ |
| Number of bunches | $n_{\rm B}$ | 2 | 4 |
| Storage turns | $n_{\rm s}$ | 1200 | 1000 |
| $\mu$-beam emittance | $\epsilon_{\rm t}$ | $0.5 \times 10^{-8}$ m rad | $10^{7}$ m rad |
| Interaction focus | $\beta_0$ | 0.1 cm | 0.5 cm |
| Beam size at interaction | $\sigma = (\epsilon_{\rm t}\beta_0)^{1/2}$ | 2.2 $\mu$m | 22 $\mu$m |

**Achnowledgments**

I warmly thank Isabelle Canon, Marinette Glomet, Susan Leech O'Neale, and Chryssafoula Rollinger for their very efficient help in the preparation of this paper.

**References**


[1] Workshop on Physics at Future Accelerators, La Thuile, 1987, CERN 87–07 (1987), talk by U. Amaldi, p. 323.

[2] ICFA Seminar at DESY, May 1993.

[3] Report of the Working Group on High Luminosities at LEP, CERN 91–02.

[4] Polarization at LEP, CERN 88–06.

[5] S. Myers and C. Wyss, LEP2 Energy Upgrade, CERN LEP2 Note 95–34.

[6] Second Workshop on Physics and Experiments with Linear $e^+e^-$ Colliders, Waikoloa, 1993, eds. F.A. Harris et al., (Singapore, World Scientific, 1993);
P. Chen et al., SLAC–PUB–5873 (1993).

[7] JLC-1, The JLC Group, KEK Report 92–16.

[8] The Large Hadron Collider: conceptual design, The LHC Study Group, CERN–AC/95–05.

[9] BABAR Letter of Intent, SLAC 443 (1994);
BELLE, KEK Report 94–2;
HERAB, DESY PRC 94/02.

[10] E. Iarocci, CERN Academic Training Lectures 1993/94.

[11] P. Renton, Rapporteur Talk at the 17th International Symposium on Lepton–Photon Interactions at High Energies, Beijing, 1995.

[12] P. Langacker et al., UPR 458T (1991).

[13] T. Sjostrand and V.A. Khoze, CERN TH 7043/93;
L. Lonnblad and T. Sjostrand, CERN TH/95–17.

[14] W.T. Stirling, DTP/95/24 (Feb. 1995).

[15] A. Blondel et al., LAPP–TH 343/91.

[16] P. Fisher et al., CERN–PPE/94–183.

[17] H. Burkhardt and B. Pietrzyk, LAPP–EXP–95–05.

[18] G. Altarelli, CERN TH 7072/93.

[19] F. Zwirner, The SUSY World, CERN–TH 6051/93;
W. De Boer, IEKP–KA/94–01 (May 1994).

[20] H. Baer et al., UCD–94–19, FSU–HEP–940501.

[21] P. Langacker and N. Polonsky, Preprint UPR–0594 T;
M. Carena and C.E.M. Wagner, CERN TH 7320/94.

[22] G. Kane et al., UM–TH–93–24.

[23] G. Altarelli and G. Isodori, CERN TH 7351/94.

[24] M. Carena et al., CERN TH/95–45, DESY 95–038, IEM–FT–103/95.

[25] J.F. Grivaz, Rapporteur Talk at the 1995 Europhysics Conference on HEP, Brussels, LAL 95–83 (Oct. 1995).

[26] Interim report on the physics motivations for an energy upgrade of LEP2, CERN–PPE/95–78, CERN TH/95–151.

[27] P. Janot, Preprint LAL 93–28.

[28] LHC Proposals: ATLAS LHCC/94–43, CMS LHCC/94–38;
F. Pauss, ETHZ–IPP PR–94–8;
J. Virdee, Preprint CMS TN/94–132.

[29] M.D. Hildreth, SLAC–PUB–6036 (1993).

[30] M. Peskin, SLAC–PUB–6582 (1994).

[31] M. Bilenky et al., Nucl. Phys. **B409** (1993) 22.

[32] R.L. Sekulin, Phys. Lett. **B338** (1994) 369.

[33] A. de Rujula et al., Nucl. Phys. **B384** (1992) 3.
[34] M.S. Chanowitz, LBL 32846, LBL 31651, LBL 32938.
[35] T.L. Barklow, SLAC–PUB–6280 (1993).
[36] R. Casalbuoni et al., Preprint UGVA–DTP 1994/03–845.
[37] V. Telnov, CLIC Note **294** (Dec. 1995) and refs. therein;
see also Proc. Workshop on Gamma–Gamma Colliders, Berkeley, 1994, Nucl. Instrum. Methods Phys. Res. **A355** (1995) 3;
Proc. 10th Int. Workshop on Photon–Photon Collisions, "Photon 95", Sheffield, UK, April 1995.
[38] F. Richard, LAL 94–45.
[39] Muon Collider Workshop, Los Alamos Report LA–UR–93–866 (1993);
R.B. Palmer, Beam Dynamics Newsletter, No. 8 (1995);
D. Cline, UCLA–CAA–0125–11/95.